Multimedia Tools and Applications (2019) 78:21853–21890
https://doi.org/10.1007/s11042-019-7498-3

An adaptive fuzzy K-nearest neighbor approach for MR brain tumor image classification using parameter free bat optimization algorithm

Taranjit Kaur[1] · Barjinder Singh Saini[1] · Savita Gupta[2]

Received: 6 August 2018 / Revised: 17 February 2019 / Accepted: 18 March 2019 /
Published online: 3 April 2019

Abstract
This paper presents an automatic diagnosis system for the tumor grade classification through magnetic resonance imaging (MRI). The diagnosis system involves a region of interest (ROI) delineation using intensity and edge magnitude based multilevel thresholding algorithm. Then the intensity and the texture attributes are extracted from the segregated ROI. Subsequently, a combined approach known as Fisher+ Parameter-Free BAT (PFreeBAT) optimization is employed to derive the optimal feature subset. Finally, a novel learning approach dubbed as PFree BAT enhanced fuzzy K-nearest neighbor (FKNN) is proposed by combining FKNN with PFree BAT for the classification of MR images into two categories: High and Low-Grade. In PFree BAT enhanced FKNN, the model parameters, i.e., neighborhood size k and the fuzzy strength parameter m are adaptively specified by the PFree BAT optimization approach. Integrating PFree BAT with FKNN enhances the classification capability of the FKNN. The diagnostic system is rigorously evaluated on four MR images datasets including images from BRATS 2012 database and the Harvard repository using classification performance metrics. The empirical results illustrate that the diagnostic system reached to ceiling level of accuracy on the test MR image dataset via 5-fold cross-validation mechanism. Additionally, the proposed PFree BAT enhanced FKNN is evaluated on the Parkinson dataset (PD) from the UCI repository having the pre-extracted feature space. The proposed PFree BAT enhanced FKNN reached to an average accuracy of 98% and 97.45%. with and without feature selection on PD dataset. Moreover, solely to contrast, the performance of the proposed PFree BAT enhanced FKNN with the existing FKNN variants the experimentations were also done on six other standard datasets from KEEL repository. The results indicate that the proposed learning strategy achieves the best value of accuracy in contrast to the existing FKNN variants.

Keywords Fuzzy K-nearest neighbor · PFree BAT optimization · Diagnosis system · Model parameters

✉ Taranjit Kaur
taran.rehal@yahoo.com; tanurehal06@gmail.com

Extended author information available on the last page of the article

1 Introduction

Brain image classification has been an active area of research for the past few years. For categorization of the abnormal brain images into low or high-grade (LG/HG), malignant/benign, etc., many feature extraction approaches have been devised in the last few years [56], and among them, the second order statistics like co-occurrence matrices and fractal attributes are most prevalent [19, 20, 28, 32, 55, 80, 83].

Zhang et al. [91] designed a mechanism for classification of the magnetic resonance (MR) brain images into normal and abnormal categories. The mechanism comprised of the stages of the feature extraction using 2D- discrete wavelet transform (DWT), followed by dimensionality reduction using principal component analysis (PCA), and classification using particle swarm optimized (PSO) Kernel support vector machine (KSVM). The parameters C and σ of the KSVM classifier were fined tuned using the PSO algorithm. Experimenting on 90 MR images from the Harvard Repository, the obtained sensitivity (*Se*), Specificity (*Sp*), and Accuracy (*Acc*) were 98.12%, 92%, and 97.78% using 1024 DWT coefficients and following a 5-fold cross-validation (CV) partitioning scheme. The attained measures were better than those obtained using Back Propagation-Neural Network (BP-NN) and Radial Basis Function (RBF)-Neural Network (RBF-NN) for which the *Acc* values were 86.22% and 91.33%. The limitation of the work was that it required a huge feature space.

Sachdeva et al. [68] developed a computer-aided diagnosis (CAD) system for the automatic segmentation and the classification of the brain tumors. The system was tested on two datasets. First comprised of 428 post-contrast T1-weighted images collected from 55 patients. The second consist of 260 MR images taken from publically available Surgical Planning Laboratory (SPL) database. The tumor regions were marked using content-based active contour (CBAC) model. From the segmented regions of interest (SROIs) intensity and texture feature set were extracted. Genetic Algorithm (GA) was used to select the optimal features. For classification, two different machine learning algorithms were used namely SVM and artificial neural network (ANN). The test results on both datasets indicated that the use of GA for the feature selection has significantly increased the classification accuracy. It has surged from 79.3% to 91.7% using SVM and using ANN it has increased to 94.9% from 74.6% for the first dataset. Similar results are reported for the second dataset where an increase from 80.8% to 89% was noticed for SVM and for the ANN the increase was from 77.5% to 94.1%. These measures were attained using a feature count of 71 and following a leave one out method (LOOM) for partitioning.

Yang et al. [88] developed a novel wavelet-energy(WE) based approach for automated classification of MR brain images as normal or abnormal using the KSVM classifier. Biogeography-based optimization (BBO) was used to optimize the weights of the SVM, i.e., regularization parameter C, scaling factor σ. The validation was done on 90 Images (5 Healthy (H), 85 Abnormal (Ab)) from the Harvard repository(http://www.med.harvard.edu/aanlib/). The attained *Se*, *Sp*, and *Acc* were 98.12%, 92.00%, and 97.78% using a total of 10 features (wavelet energies from the 10 sub-bands decomposed using Haar wavelet) and following 5×5 fold CV partitioning scheme. The attained metrics were better than that obtained using WE

and KSVM without optimization for which the *Se*, *Sp*, and *Acc* were 93.18%, 68.00%, and 91.78%. The performance was sensitive to the choice of the mother wavelet and the number of decomposition levels. Better value of the accuracy measure can be expected by employing efficient feature descriptors, such as scale-invariant features and using some advanced pattern recognition techniques.

Skogen et al. [72] designed a mechanism for distinguishing HG from LG glioma based on the exploration of MR image texture information. The mechanism encompasses demarcation of the tumorous region manually tailed by the utilization of the filtration histogram method. This method subjects the segmented region to a filtering process by applying a Laplacian of Gaussian band-pass filter that is then employed to excerpt the attributes at the different size of the spatial scale filter. Evaluation on 67 HG and 27 LG glioma subjects indicated that standard deviation at the fine texture scale was the best distinguishing feature resulting in a *Se* of 81% and a *Sp* of 93%.

Lu et al. [52] proposed a novel approach for MR image classification that employed 2D-DWT and calculated the entropies of the sub-bands that served as features. Thereafter, a BAT algorithm optimized ELM (BA-ELM) was trained to classify pathological brains from healthy controls. BAT algorithm was employed to fine-tune the weights/biases and the parameters of the hidden layer. The experimentation was done on 132 MR brain images Harvard Medical School Repository that comprised of 18 H and 114 Ab MR Images. Using a total of 7 features and following a 10×10 fold CV, the obtained *Se*, *Sp*, and *Acc* were 99.04%, 93.89%, and 98.33%. The results were better than that obtained by other classifiers like SVM, Naive Bayes, and RBFNN for which the *Acc* values were 95%, 92.60%, and 91.33%. The drawback of the approach was that it required empirical tuning of the number of the hidden neurons and the type of wavelet used for the decomposition.

Lahmiri [38] compared three automatic diagnosis schemes for the categorization of the normal subjects from glioma patients. The MR images used for categorization were obtained from the Harvard Medical School Repository. The images comprised of 50 T2-w MR scans in axial orientation out of which 20 were abnormal brains affected with glioma and 30 were normal brains. The diagnosis scheme involved four stages: Firstly, the conventional PSO, Darwinian PSO (DPSO), or fractional order DPSO (FODPSO) were used for the segmentation of the MR image. Secondly, for the segmented regions directional spectral distribution (DSD) was calculated. Thirdly, multifractals of the DSD (also called as multi-scale analysis (MSA)) were computed that constituted the feature vector. Lastly, the categorization was done using SVM with LOOM partitioning scheme. The FODPSO+DSD + MSA + SVM scheme provided the finest results using 6 features. This scheme resulted in an *Acc* value of 99.18% with *Se* and *Sp* of 100% and 97.95% respectively.

Bahadure et al. [4] devised CAD technology for the automatic segmentation and classification of tumorous MR images. The CAD consists of stages of pre-processing that involved contrast enhancement and skull stripping, segmentation, feature extraction, feature selection, and classification. For segmentation, different techniques were adopted that involved watershed segmentation, Fuzzy C Means, Discrete Cosine Transformation, and Berkley Wavelet Transform. Feature extraction involved extracting first order statistics, features from gray level co-occurrence

matrix(GLCM), and the tumor area. The features were reduced using the GA algorithm, and the tumor classification was done using adaptive neuro-fuzzy inference system, K-Nearest Neighbors (K-NN), and GA based approach. The experimentation involved 135 tumorous and 67 normal images. A comparative analysis was also done using the aforesaid segmentation and classification approaches. Best results were obtained by employing a Berkley Wavelet Transform for segmentation and adopting a GA based classification scheme. The experimental results achieved *Se* of 92.36%, *Sp* of 91.42%, and *Acc* of 92.03% for the task of normal versus tumor classification.

Hemanth et al. [26] devised modified GA for the classification of the abnormal MR brain tumor images. The reproduction operators of GA algorithm were modified to generate new offspring. Thereafter the modified versions were used for feature selection. The validation was done 450 T2-w images collected from the private scan center comprising of the categories of meningioma, metastase, glioma, and astrocytoma. Gray level Difference matrix was used to extract features from these images. A total of 14 features were extracted which were further reduced to 9 using GA1. These reduced features were fed to the Back Propagation neural network for classification. The obtained *Se*, *Sp*, and *Acc* values were 96%, 98%, and 98.1% using a fixed partition scheme (120: Training, 330: Testing).

Gupta et al. [22] developed a glioma detection system based on the texture and the morphological features coupled with ensemble learning. The system worked at three different levels. At the first level, the tumor was segmented using adaptive thresholding or canny edge detection technique followed by morphological operation. At the second level, its location was analyzed and it was classified as super-tentorial or Infra-tentorial. At the third level of classification, the tumor type was identified based on the morphological and other inherent characteristics like area, perimeter, solidity, and the orientation as features through an ensemble of SVM, KNN, and Naïve Bayes (NB) classifiers. Experimentation was done on BRATS 2012 dataset, taking 120 HG, 80 LG images in all the four sequences. The obtained *Acc* using a 10-fold CV was 94.40/94% for LG/HG using T1 and T1-CE Images. Using FLAIR and T2-w images, following a 10-fold CV, the attained *Acc* was 96.5/97%. The limitation of the developed system was that it needs preprocessing stages of cropping and enhancement.

Optimization techniques have always played a vital role in the design of the CAD system be it be feature selection or for tuning the model parameters of the classifier [4, 26, 52, 68, 72, 88, 91]. Empirically tuning the model parameters of the classifier is a computationally complex task. To ease this complexity and to improvise the accuracy, optimization techniques have been often used to fine-tune the model parameters of the machine learning algorithms especially for medical diagnosis [50, 52, 71, 73, 88, 91]. Improper model or kernel parameters lead to poor generalization performance of the algorithms.

Prominently, the algorithms like PSO, BBO, and BA have been often employed to optimize the model parameters of the KSVM, i.e., C and σ or weights/biases of the hidden layer of the ELM algorithm and thereafter use it for MR image classification [52, 88, 91]. But none of the algorithms have used PFree Bat Algorithm for optimizing the neighborhood size *k* and the fuzzy strength parameter *m* of the Fuzzy K-nearest neighbor (FKNN) classifier.

Moreover, most of the CAD system dealing with tumor classification (either normal versus abnormal or high grade/low grade or multiclass classification) discussed above have validated their system on either the benchmark dataset from the Harvard repository or on their own self-collected private datasets [4, 26, 38, 52, 68, 72, 88, 91]. Very few works like that in [22] have addressed the tumor grade classification using the BRATS 2012 dataset.

The work is motivated by the excellent performance achieved by the FKNN classifier on disease diagnosis like thyroid [50] and the Parkinson [8, 73]. In this paper, an attempt has been made to investigate the efficacy of PFree BAT enhanced FKNN classifier in constructing an automatic system for diagnosis of the abnormality like tumors in MR images.

In this present work, we have designed PFree enhanced FKNN classifier by adaptively tuning the neighborhood size k and the fuzzy strength parameter m of the FKNN classifier using the PFree BAT optimization algorithm. PFree BAT algorithm is an improvised version of the BAT algorithm that combines the major strengths of the BAT and the parameter Free PSO algorithm. Thereafter, the PFree enhanced FKNN classifier is integrated with the initial stages of segmentation, feature extraction, and the feature selection to form a CAD system. The CAD system consists of four major modules.

In the first module segregation of the complete tumor is done by the intensity and the edge magnitude based multilevel thresholding approach [34]. The delineated tumor regions are saved as segmented regions of interest (SROIs). In the second module, intensity and texture features are extracted from the SROIs [33, 35]. In the third module, feature selection is done using Fisher and the PFree BAT optimization algorithm [35]. The selected features are then used as inputs to the PFree BAT enhanced FKNN classifier whose model parameters are fine-tuned using the PFree BAT optimization algorithm. Finally, the classification module consists of classifying brain tumor class as HG or LG by using the enhanced FKNN model.

The designed CAD has been extensively validated on tumor images taken from the BRATS 2012 dataset and on three versions of datasets taken from the Harvard Repository.

As the work primarily focuses on the optimizing the neighborhood size k and the fuzzy strength parameter m of the FKNN classifier through PFree BAT optimization algorithm, so the performance is validated on the benchmark Parkinson dataset from the UCI machine learning repository and six other standard datasets from KEEL repository having pre-extracted feature space. Such experimentation has been explicitly undertaken to highlight the strength of the PFree enhanced FKNN classifier in the absence of the previous stages like segmentation, feature extraction, and selection. The proposed scheme is compared with standard KNN and different optimized version of the FKNN. The comparison is statistically validated using the paired t-test and the Friedman statistical significance test. Furthermore, the comparison with the existing state of the art has also been done.

To summarize the key contributions of the paper are as follows:

1. Firstly, the main contribution of the paper is proposing a new FKNN parameter tuning scheme that uses PFree BAT algorithm. The full potential of the FKNN classifier is explored by the use of the PFree BAT algorithm that determines the optimal value of parameters k, and m in FKNN. Integrating PFree BAT with FKNN enhances the classification capability of FKNN.

2. Secondly, a simple and effective solution is proposed for grading of glioma into low and the high-grade categories by integrating an automatic segmentation method [34], feature extraction approach [33, 35], feature selection algorithm [35], and the proposed PFree enhanced FKNN model.
3. Extensive experimentations have been conducted on the different datasets like those from BRATS 2012, Harvard Repository (3 Versions of the datasets), Parkinson data set from UCI machine learning repository, and six benchmark datasets from KEEL repository. Experimentation on the datasets from the UCI and KEEL repository have been explicitly undertaken to validate the performance of PFree BAT Enhanced FKNN on the pre-extracted feature space. The proposed scheme is compared with standard KNN and different optimized version of the FKNN. The comparison is statistically validated using the paired t-test and the Friedman statistical significance test. Moreover, for every dataset comparison with the recent existing state of art methods is also done.

Paper organization: The paper is structured as follows; Section 2 provides the mathematical background of the related methodologies, Section 3 describes the proposed methodology, Section 4 details the datasets and the evaluation criteria, Section 5 gives the experimental results, Section 6 provides the discussion, and finally, the conclusion is given in the last section.

2 Mathematical backgrounds of the related methodologies

The work presented in this paper is primarily focused on the optimizing the neighborhood size k and the fuzzy strength parameter m of the FKNN classifier through PFree BAT optimization algorithm. This section is devoted to the theoretical background of FKNN and the PFree BAT optimization algorithm.

2.1 Fuzzy k-nearest neighbor method (FKNN)

Fuzzy K-NN adds the concept of the fuzzy logic into the conventional K-NN classifier. Rather than assigning a crisp value of 0 or 1 to a sample vector, it assigns membership to the sample vector. The basis of the FKNN algorithm is to assign the membership as a function of the sample vector's distance from its K-nearest neighbors and those neighbors' class memberships in the possible classes.

The fuzzy memberships for the sample vectors are assigned to different classes as per the following formula [36]:

$$u_i(x) = \frac{\sum_{j=1}^{k} u_{ij}\left(\frac{1}{\left\|x-x_j\right\|^{\frac{2}{m-1}}}\right)}{\sum_{j=1}^{k}\left(\frac{1}{\left\|x-x_j\right\|^{\frac{2}{m-1}}}\right)} \tag{1}$$

Where $j = 1,2,\ldots\ldots,k$, and $i = 1,2\ldots\ldots..C$, with k as number of nearest neighbors and C as the number of classes, m denotes the fuzzy strength parameter that decides how heavily the distance is weighted when computing the contribution of each neighbor to the membership value. The $\|x - x_j\|$is the Euclidean distance between x and its j^{th} nearest neighborx_j. The u_{ij}

denotes the membership degree of the pattern $x_j$of the training set to the class i. There are different ways in which u_{ij}can be defined. One works by assigning crisp membership to each training pattern, i.e., the training patterns possess whole membership in their particular class and non-membership in all other classes. The other way works by assigning constrained fuzzy membership, i.e., the k nearest neighbors of each training sample vector are found, and the membership of x_k in each class is assigned as [36]:

$$u_{ij}(x_k) = \left\{ \begin{array}{c} 0.51 + \frac{n_j}{K} \times 0.49, \quad if \ j = i \\ \frac{n_j}{K} \times 0.49, \quad if \ j \neq i \end{array} \right\} \tag{2}$$

In eq. (2) n_j specify the number of the neighbors belonging to the j^{th} class. The membership computed via eq. (2) must satisfy the equations as follows [36].

$$\sum_{i=1}^{2} u_{ij} = 1, \qquad j = 1, 2, ..., n \tag{3}$$

Where

$$u_{ij} \in [0, 1]$$

In our preliminary experimentation, the first mechanism, i.e., the fuzzy classifier with crisp initialization had resulted in improved classification accuracy than with the constrained initialization.

For any query sample, the membership value u_i is computed for all the classes under consideration, and after that, it is allocated to the class to which it possesses the highest membership, i.e.,

$$c(x) = \arg[\max(u_i(x))]_{i=1}^{2} \tag{4}$$

2.2 Parameter free BAT (PFree BAT) optimization algorithm

Bat Algorithm (BAT) introduced by Yang [84] is the latest meta-heuristic optimization algorithm inspired by the echolocation skill of the microbats which directs them on their foraging behavior. The BAT is an amalgamation of the major strengths of the PSO and Harmony Search algorithm.

Every bat follows certain procedures for the position (x_i) and velocity (v_i) updating at each time step, t, in accordance with the pulse frequencyQ_i. The details regarding the conventional BAT algorithm can be found in the works by [84]. The newer solutions are generated by following a set of equations as given below [84]:

$$Q_i = Q_{\min} + (Q_{\max} - Q_{\min})\beta \tag{5}$$

$$v_i^t = v_i^{t-1} + \left(x_i^{t-1} - x^*\right) Q_i \tag{6}$$

$$x_i^t = x_i^{t-1} + v_i^t \tag{7}$$

$$x_{new} = x_{old} + \varepsilon A^t \tag{8}$$

$$A_i^{t+1} = \alpha A_i^t \tag{9}$$

$$r_i^{t+1} = r_i^0 (1 - \exp(-\gamma t)) \tag{10}$$

The exploitation and exploration capabilities of the conventional BAT algorithm are indigent [89]. To counteract with this limitation, the modification structure was proposed, inspired by the study in [5, 64]. The bat locations are directly updated through a new position update equation as illustrated below [35]:

$$x_i^t = \left(1 - \frac{x^*}{x_i^{t-1}}\right) \times Q_i \times x^* + \left(\frac{x^*}{x_i^{t-1}}\right) \times Q_i \times pbest_i \tag{11}$$

The improved version of position update equation guides the bat under the influence of the $x^*$and the previous best solution ($pbest_i$). As the modified Bat algorithm eliminates the velocity update equation, so it is termed as PFree BAT Algorithm. Better performance of the proposed PFree BAT optimization algorithm has been ascertained by experimenting on standard benchmark functions as reported in our previous works [35].

3 Proposed methodology

The flowchart of the CAD system incorporating the proposed PFree BAT enhanced FKNN classifier for tumor grade classification (HG/LG) is shown in Fig. 1. The step by step procedure of how the CAD operates is briefed as Algorithm 1.

Algorithm 1 CAD system incorporating the proposed PFree BAT enhanced FKNN classifier for MR image classification	
***Input*:**	*MR Image Dataset from BRATS 2012 dataset/Harvard Repository Dataset*
***Output*:**	*Tumor Grade (HG/LG: BRATS Dataset) or (H/Glioma or H/Ab: Harvard Dataset)*
***Step1*:**	*Segment the whole tumor region from the FLAIR images using the Intensity and edge magnitude-based multilevel thresholding algorithm* [22]
***Step 2*:**	*Map out the FLAIR segmented region onto T1-contrast and T1 images and then compute their difference* [23]
***Step 3*:**	*From the difference image generated at Step 2 compute various intensity and texture attributes that include the First Order Statistics, GLCM, GLRM, GTDM, LTF, Fractal, Gabor Filter/wavelet-based, and EMD based features*[24]
***Step 4*:**	*The dimensionality of the normalized feature set extracted in Step 3 is reduced by adopting the Fisher Criterion and PFree BAT optimization algorithm*[24]
***Step 5*:**	*The reduced feature space is fed to the proposed* ***PFree BAT enhanced*** *FKNN classifier using a five-fold cross-validation partitioning scheme. The predicted class labels for test set are then used to calculate the classifier performance measures*

The CAD system as shown in Fig. 1 primarily comprises of Tumor segmentation, Slice selection, Feature extraction, Feature Selection, and the Classification using the proposed PFree BAT enhanced FKNN classifier.

3.1 Tumor segmentation

The complete tumor region is segmented from the Fluid-attenuated inversion recovery (FLAIR) images using the Intensity and edge magnitude-based multilevel thresholding [34] technique. This technique exploits both intensity and edge

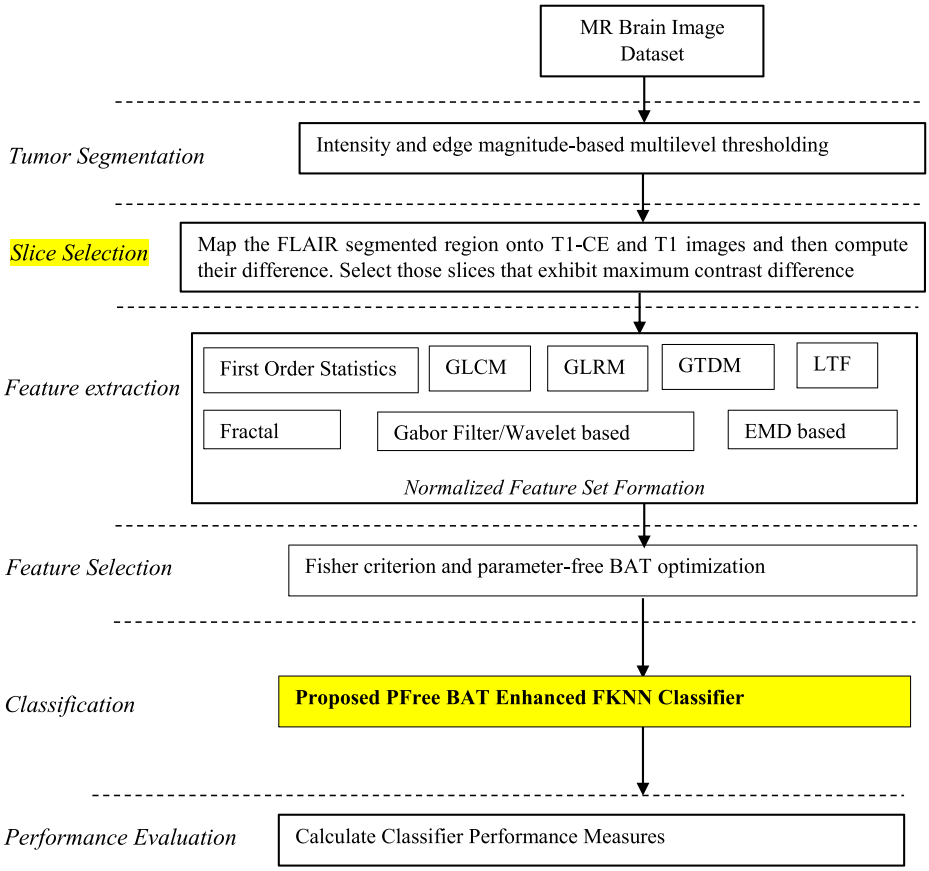

Fig. 1 Flowchart of the proposed diagnosis system

magnitude information present in image histogram and GLCM to compute the multiple thresholds through an optimization procedure which are then used for segmentation.

3.2 Slice selection

Following, the process of tumor segmentation, the segregated tumor region was mapped onto the T1-Contrast and the T1-w images. Thereafter, the difference image was generated. Those slices were selected for further processing that exhibited maximum contrast difference [33].

3.3 Feature extraction

A total of 52 features were extracted from the difference image by applying the standard texture models. These include the First-Order Statistics, Gray Level Co-occurrence Matrix (GLCM) [24, 79], Gray Level Run Length Matrix (GLRM) [76], Gray Tone Difference Matrix (GTDM) [1], Law's Texture Features (LTF) [77],

Fractal [12], Gabor Filters [29], Gabor Wavelet [31], and the Empirical mode decomposition (EMD) [11] based features. After extracting the feature vector, normalization was done to standardize all the features to the same level, i.e., in the range between [0 1].

3.4 Feature selection

After extraction of these 52 attributes, feature selection method formulated by fusion of Fisher and the PFree BAT optimization algorithm was applied resulting in the selection of the most informative attributes [35]. The parameters for the PFree BAT algorithm have been chosen after experimenting on the training data that results in maximum classification accuracy in the minimum amount of time with a minimal number of features.

3.5 Classification

The selected features were then fed to the classifier for the final label prediction. The two parameters, i.e., $\boldsymbol{k}$, $\boldsymbol{m}$ of the FKNN classifier greatly affect the classification accuracy. However, the selection of the appropriate values of these parameters is a tedious task. Therefore, PFree BAT optimization algorithm is used to search for the optimal combinations of the parameters of FKNN. So a PFree BAT enhanced FKNN classifier is designed in the present work in which $\boldsymbol{k}$, $\boldsymbol{m}$ of the FKNN classifier are fine-tuned by PFree BAT algorithm.

The individual bat positions in PFree BAT enhanced FKNN classifier contains a value of $\boldsymbol{k}$, and $\boldsymbol{m}$ and they are initialized in the range between 1 to 10. The average classification accuracy measure is taken into consideration while constructing the fitness function and is mathematically given as

$$g = mean(Accuracy) = \frac{\sum_{fold=1}^{3} test\left(Accuracy_{fold}\right)}{3} \tag{12}$$

where $mean(Accuracy)$ in the above expression for g indicates the average testing accuracy attained by the FKNN classifier via k-fold CV, where $k = 3$. A 3-fold CV has been employed for the model parameter selection that is different from the outer loop of 5-fold CV, that is utilized for performance computation. Such an explicit combination has been taken by empirically computing the value of the performance metrics for the different combination of folds in the outer and the inner loop. The pseudocode for the inner parameter optimization is given as Algorithm 2 that comprehensively elaborates how the proposed PFree enhanced FKNN classifier computes the optimal values for the $\boldsymbol{k}$, and $\boldsymbol{m}$.

The PFree BAT obtains the optimal solution after a series of iterative computation. The detailed iterative procedure is given as a flowchart in Fig. 2. In the PFree BAT algorithm, the following values are initialized as population size $(N) = 10$, no. of generation of bats $= 10$, loudness$(A_i) = 0.2$, emitting sound pulse rate (r_i) $=0.4$, minimum frequency$Q_{\min}$=0 and maximum frequency$Q_{\max}$=2. To obtain the best classification results for characterization of the tumors or abnormal MR Images, the overall accuracy has to be maximized.

Algorithm 2 Pseudo-code for Inner Parameter Optimization Procedure

Step 1 :	Initialize the different parameters of the BAT algorithm as population size (N) =10, no. of generation of bats =10, loudness (A_i)=0.2, emitting sound pulse rate (r_i) =0.4, minimum frequency $Q_{\min}$ =0 and maximum frequency $Q_{\max}$ =2
Step 2:	Randomly generate the initial BAT positions that encode the parameters ***k*** and ***m***. Both these parameters are initialized in the range between 1 to 10.
Step 2.1	Train the FKNN using ***m*** and rounded ***k*** via 3- fold cross-validation
Step 2.2	Predict class labels for the test set using trained FKNN model using the following equations $c(x) = \arg[\max(u_i(x))]_{i=1}^{2}$ where $u_i(x) = \frac{\sum_{j=1}^{k} u_{ij}\left(\frac{1}{\|x - x_j\|^{\frac{2}{m-1}}}\right)}{\sum_{j=1}^{k}\left(\frac{1}{\|x - x_j\|^{\frac{2}{m-1}}}\right)}$ j=1,2,…,k, and i=1,2…..,C
	with ***k*** as the number of nearest neighbors and ***C*** as the number of classes, ***m*** denotes the fuzzy strength parameter
Step 3:	Compute the fitness value as $g = mean(Accuracy) = \frac{\sum_{fold=1}^{3} test(Accuracy_{fold})}{3}$ and select the $pbest_i$ for every BAT and the ***gbest*** for all BATs. Initially, $pbest_i$ is equal to BAT position and ***gbest*** =BAT position having maximum fitness. i.e., the maximum value of g
Step 4:	Update the generation value
Step 5:	Update the position of each BAT using $x_i^t = (1 - \frac{x^*}{x_i^{t-1}}) \times Q_i \times x^* + (\frac{x^*}{x_i^{t-1}}) \times Q_i \times pbest_i$; i refers to the current BAT position
Step 6:	Is rand (0,1) > pulse rate (r_i), If yes go to Step 7 else go to Step 8 to generate new solutions
Step 7:	Produce a local solution by exploiting around the best solution $x_{new} = x_{old} + \varepsilon A_i^t$
Step 8:	Generate a new solution by flying randomly If ($rand$ (0,1) < A_i && $cfit_i > gfit$) current fitness: ***cfit$_i$***, fitness value of ***gbest***: ***gfit*** Accept the new solutions Increase r_i and decrease A_i or take constant values of r_i and A_i end
:Step 9:	Recalculate the fitness value as $g = mean(Accuracy) = \frac{\sum_{fold=1}^{3} test(Accuracy_{fold})}{3}$ for new solutions
Step 10:	Update the ***pbest$_i$*** value by comparing the fitness value of the new solutions (current fitness: ***cfit$_i$***) with the fitness value of the pbest's (***pfit$_i$***) If (***cfit$_i$*** > ***pfit$_i$***) ***pfit$_i$*** = ***cfit$_i$***; ***pbest$_i$*** =current BAT position end
Step 11:	Check if the updation is done for all the BAT's. If yes, go to Step 12 else go to Step 5
Step 12:	Update the ***gbest*** value by comparing the fitness value of ***gbest*** (***gfit***) with ***pfit$_i$*** of the whole population If (***pfit$_i$*** > ***gfit***) ***gbest***= ***pbest$_i$***; end
Step: 13	Check if the stopping criteria, i.e., end of generations reached. If yes go to Step 14 else go to Step 4
Step 14:	Get the optimal value of the parameters from ***gbest*** ***k_opt***=round(***gbest*(1)**) ***m_opt*=*gbest*(2))**

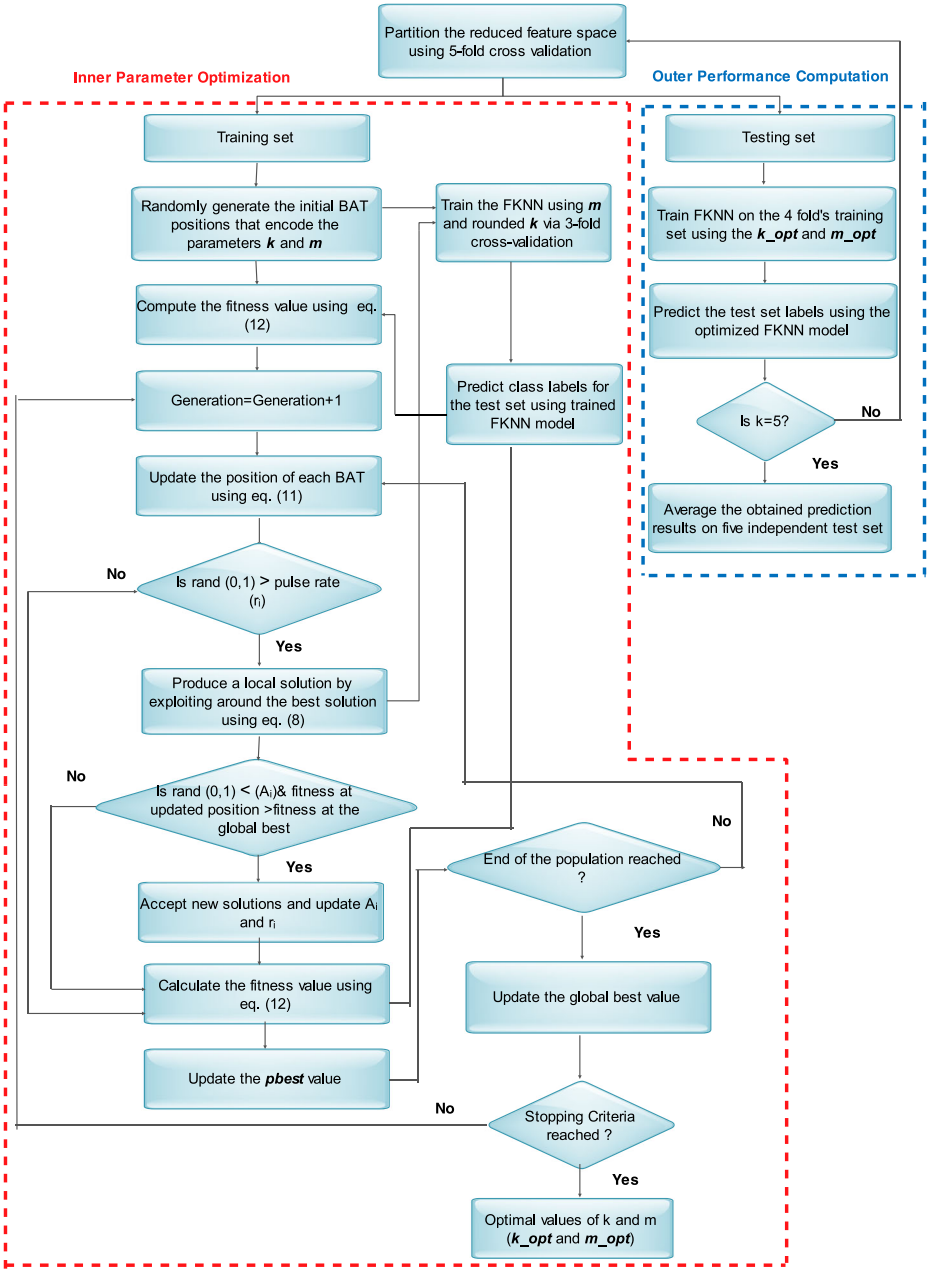

Fig. 2 Detailed procedure of the proposed PFree BAT enhanced FKNN system

4 Datasets and the evaluation criteria

4.1 Datasets

The proposed CAD system employing the PFree BAT enhanced FKNN classifier has been validated on tumor images procured from BRATS 2012 database [58]. The dataset encompassed of the real low and high-grade glioma volumes. From the training volumes, after the segmentation process, a slice selection procedure was applied. In the slice selection procedure, the complete abnormal region that has been delineated from the FLAIR set of images [34] was then mapped onto the T1 and T1-CE images. From the mapped out area, an image was created by differencing T1 and T1-CE intensity levels [33]. Only those segmented slices were taken for the further processing that exhibited a significant contrast difference. In the present work a total of 120 such difference images were taken (60 HG and 60 LG).

The latest datasets, i.e., BRATS 2013/2015 also contain the cases continued from BRATS 2012 with slight variations in the labelling of the ground truth (more labels are included in the ground truth of BRATS 2013 dataset) and reduction in the number of image slices (For the same case the slices are reduced in BRATS 2015 dataset).

To the best of the author's knowledge, only limited works have addressed tumor grade classification problem using the BRATS 2012 dataset [22]. In order to facilitate fair comparison with other recent works on brain image classification, experiments were also conducted on images obtained from the Harvard medical school repository apart from solely employing the BRATS 2012 Dataset. Three versions of the dataset from the Harvard repository have been used. The Version 1 [38] comprises of 50 T2-weighted MR brain images including 30 images of normal (healthy) brains and 20 of abnormal (unhealthy) brains affected with glioma tumor. Version 2 [59] consist of 66 T2-weighted MR brain images out of which 18 were normal, and 48 were abnormal containing cases of Glioma, Alzheimer, Metastatic bronchogenic carcinoma, Herpes encephalitis, and Multiple sclerosis. Version 3 [59] encompasses 160 T2-weighted MR brain images out of which 20 were normal and 140 were abnormal. The abnormal class has images of glioma, meningioma, Alzheimer's disease, Alzheimer's disease plus visual agnosia, Pick's disease, sarcoma, and Huntington's disease.

Additionally, the versatility of the proposed PFree BAT enhanced FKNN model has been validated on benchmark Parkinson dataset (PD) from the UCI repository (http://archive.ics.uci.edu/ml/machine-learning-databases/parkinsons/, last accessed: September 2016) having fixed set extracted feature space. This dataset consists of biomedical voice measurements from 31 people out of which 23 had PD. Each column entry in the data file denotes a distinct voice measure (comprising of a total of 22 features), and each row corresponds to one of 195 voice recording. The main objective of the data is to distinguish healthy subjects from those having PD, according to the "Status" column that is set to 0 for healthy and 1 for PD.

Moreover, the performance of the proposed PFree BAT enhanced FKNN model has been tested on six benchmark datasets taken from KEEL repository (http://www.keel.es/datasets.php) solely to contrast the performance ability of the proposed PFree BAT enhanced FKNN model with other existing FKNN variants as reported in the works by Derrac et al. [16]. The table below details the datasets employed in the present work. (Table 1).

Table 1 Summary of the datasets used for the validation of the proposed CAD

Dataset	No. of Images /Samples	Segmentation Oriented	Segmentation Free	Feature Extraction Needed	Feature Selection Needed	Proposed PFree BAT Enhanced FKNN classifier	Output
BRATS 2012	120	✓	✖	✓	✓/✖	✓	Low Grade vs High grade glioma
Harvard Repository Version 1	50	✖	✓	✓	✓	✓	Normal vs glioma
Harvard Repository Version 2	66	✖	✓	✓	✓	✓	Normal vs Abnormal Brains
Harvard Repository Version 3	160	✖	✓	✓	✓	✓	Normal vs Abnormal Brains
Parkinson Disease (PD) Data from UCI Repository	195 voice recording with 22 features	✖	✖	✖	✓/✖	✓	Normal vs PD
Appendictis from KEEL Repository	106 Instances with 7 attributes	✖	✖	✖	✓	✓	2 Classes (patient has appendicitis or not)
Bupa from KEEL Repository	345 Instances with 6 attributes	✖	✖	✖	✓	✓	2 Classes (individual suffers from alcoholism or not)
Heart from KEEL Repository	270 Instances with 13 attributes	✖	✖	✖	✓	✓	2 Classes (absence or presence of heart disease)
Hepatitis from KEEL Repository	80 Instances with 19 attributes	✖	✖	✖	✓	✓	2 Classes (Patient with Hepatitis will die or survive)
Monk-2 from KEEL Repository	432 Instances with 6 attributes	✖	✖	✖	✓	✓	2 Classes (Class 0 and Class 1)
Wdbc from KEEL Repository	569 Instances with 30 attributes	✖	✖	✖	✓	✓	2 Classes (Benign or malignant tumor)

✓/✖: Results are computed with and the without feature selection mechanism

4.2 Evaluation criteria

The well-known classification metrics of Sensitivity(*Se*), Specificity(*Sp*), and Accuracy(*Acc*) have been chosen to measure the proficiency of the proposed diagnosis system. These measures are widely utilized for the application of the disease diagnosis. These measures comprise of True Negative (*TN*), False positive (*FP*), True Positive (*TP*), and False Negative (*FN*). *TN* means the cases of the low-grade glioma that are correctly categorized as low-grade, *FP* is the number of the low-grade cases categorized as high-grade. *TP* is the number of the high-grade tumors correctly categorized as high-grade, and *FN* is the number of high-grade tumors incorrectly categorized as low-grade. Numerically, *Se* and *Sp* are defined as [40].

$$Se = \frac{TP}{TP + FN} \tag{13}$$

$$Sp = \frac{TN}{TN + FP} \tag{14}$$

$$Acc = \frac{TN + TP}{TP + FP + TN + FN} \tag{15}$$

Thereafter, the *Acc* which reflects the complete detection rate is computed as.

In addition to the *Se*, *Sp*, and *Acc*, the area under the receiver operating characteristic (ROC) curve, i.e., *Auc* and the Mathew correlation coefficient (*Coeff*) are also computed. For computing Auc, the method proposed in [18] was used. The *Coeff* was directly calculated by the formula given below

$$Coeff = \frac{TN \times TP - FP \times FN}{\sqrt{(TP + FP)(TP + FN)(TN + FP)(TN + FN)}} \tag{16}$$

5 Experimental results

The result section has been primarily focused on the analysis of the brain tumor images from BRATS 2012 dataset using the quantitative performance measures. It is supplemented by comparison with conventional KNN and several optimized FKNN models. The quantitative comparison is tailed by statistical verification by the paired *t*-test. The section also highlights the classification performance of the proposed PFree BAT enhanced FKNN with and without the feature selection mechanism.

5.1 Comparison of the proposed CAD with different optimized FKNN models

Table 2 reports the results using the various performance metrics, i.e., *Se*, *Sp*, *Acc*, *Auc*, and *Coeff* on BRATS 2012 brain tumor dataset [58] using different optimization algorithms like Real-Coded Genetic Algorithm (RGA), PSO, biogeography-based optimization (BBO), Cuckoo Search [86, 87], Firefly Algorithm, Improved Harmony Search [54], BAT Algorithm [84],

Table 2 Se, Sp, Acc, Auc, and Coeff for the tumor dataset using various optimization algorithms

Method for feature selection	Algorithm used for the classifier parameter optimization	Performance Metrics	Conventional KNN Metrics (SD)	Adaptive FKNN or PFree enhanced FKNN Metrics(SD)	Statistical Significance using the paired *t*-test (*p* value)
Fisher + RGA	RGA	*Se*	0.9556 (0.0994)	1 (0)	0.0315
		Sp	0.9600 (0.0548)	0.9800 (0.0447)	
		Acc	0.9579 (0.0440)	0.9895 (0.0235)	
		Auc	0.9700 (0.0447)	0.9900 (0.0224)	
		Coeff	0.9418 (0.0859)	0.9800 (0.0447)	
Fisher + PSO	PSO	*Se*	0.9333 (0.0994)	0.9333 (0.0994)	0.0043
		Sp	0.9400 (0.0548)	0.9600 (0.0548)	
		Acc	0.9368 (0.0686)	0.9474 (0.0744)	
		Auc	0.9367 (0.0459)	0.9478 (0.0374)	
		Coeff	0.8788 (0.0853)	0.8976 (0.0747)	
Fisher + BBO	BBO	*Se*	0.9111 (0.1217)	0.9333 (0.0994)	0.0222
		Sp	0.9200 (0.1095)	0.9800 (0.0447)	
		Acc	0.9158 (0.0471)	0.9579 (0.0440)	
		Auc	0.9267 (0.0460)	0.9367 (0.0678)	
		Coeff	0.8574 (0.0942)	0.8753 (0.1359)	
Fisher + Cuckoo Search [86, 87]	Cuckoo Search [86, 87]	*Se*	0.9111 (0.1217)	0.9556 (0.0609)	0.0018
		Sp	0.9400 (0.0548)	0.9200 (0.0837)	
		Acc	0.9263 (0.0600)	0.9368 (0.0440)	
		Auc	0.9367 (0.1131)	0.9578 (0.0678)	
		Coeff	0.8753 (0.2265)	0.9176 (0.1351)	
Fisher + Firefly Algorithm [74]	Firefly Algorithm [74]	*Se*	0.8667 (0.1449)	0.9333 (0.0994)	0.0139
		Sp	0.9200 (0.1789)	0.9600 (0.0894)	
		Acc	0.8947 (0.0832)	0.9474 (0.0526)	
		Auc	0.8944 (0.0543)	0.9267 (0.0711)	
		Coeff	0.7958 (0.1073)	0.8567 (0.1390)	
Fisher + Improved Harmony Search [54]	Improved Harmony Search [54]	*Se*	0.9556 (0.0994)	0.9556 (0.0994)	0.00227
		Sp	0.8800 (0.1304)	0.9600 (0.0894)	
		Acc	0.9158 (0.0956)	0.9579 (0.0942)	
		Auc	0.9178 (0.0270)	0.9600 (0.0418)	
		Coeff	0.8412 (0.0538)	0.9218 (0.0805)	
Fisher + BAT Algorithm [84]	BAT Algorithm [84]	*Se*	0.9333 (0.0609)	0.9778 (0.0497)	0.0133
		Sp	0.9400 (0.0548)	0.9600 (0.0548)	
		Acc	0.9368 (0.0440)	0.9684 (0.0288)	
		Auc	0.9356 (0.0231)	0.9578 (0.0442)	
		Coeff	0.8771 (0.0493)	0.9176 (0.0878)	
Fisher + Novel BAT with Habitat Selection [57]	Novel BAT with Habitat Selection [57]	*Se*	0.9111 (0.0930)	0.9556 (0.0609)	0.0357
		Sp	0.9600 (0.0548)	0.9800 (0.0447)	
		Acc	0.9368 (0.0577)	0.9684 (0.0288)	
		Auc	0.9256 (0.0624)	0.9356 (0.0589)	
		Coeff	0.8581 (0.1186)	0.8766 (0.1129)	
Fisher+ DE [10, 78]	DE [10, 78]	*Se*	0.9333 (0.0609)	0.9778 (0.0497)	0.0111
		Sp	0.8800 (0.1304)	0.9000 (0.1414)	
		Acc	0.9368 (0.0686)	0.9368 (0.0686)	
		Auc	0.9067 (0.0659)	0.9389 (0.0650)	
		Coeff	0.8205 (0.1317)	0.8865 (0.1206)	
Fisher + Time variant PSO [7]	Time variant PSO [7]	*Se*	0.9556 (0.0609)	0.9556 (0.0994)	0.0035
		Sp	0.9400 (0.0894)	0.9600 (0.0548)	
		Acc	0.9474 (0.0645)	0.9579 (0.0686)	
		Auc	0.9478 (0.0635)	0.9578 (0.0699)	
		Coeff	0.8976 (0.1270)	0.9171 (0.1365)	
Fisher + PFree BAT Algorithm (Proposed)	PFree Bat Algorithm (Proposed)	*Se*	1(0)	1(0)	Ref*
		Sp	0.9800 (0.0447)	1(0)	
		Acc	0.9895 (0.0235)	1(0)	
		Auc	0.9900 (0.0224)	1(0)	
		Coeff	0.9800 (0.0447)	1(0)	

Se: Sensitivity

Sp: Specificity

Acc: Accuracy

Auc: Area under the curve

Coeff: Mathew correlation coefficient

RGA: Real Coded GA; PSO: Particle Swarm Optimization; BBO: Biogeography Based Optimization; DE: Differential Evolution; PFree BAT: Parameter Free BAT

*Ref: *p* values are calculated w.r.t the proposed method

Novel BAT with Habitat Selection [57], Differential Evolution (DE) [10, 78], Time-variant PSO [7], and the proposed PFree Bat algorithm. The standard deviation values accompany these metrics in the brackets.

These metrics were computed after feature selection and the parameter optimization stage. For the feature selection, the optimization algorithm was used in conjunction with Fisher criteria to choose the most discriminatory subset of attributes. The reduced feature set was then given as training input to the FKNN classifier whose parameters were optimized using the various meta-heuristic algorithms as detailed in Table 2. The MATLAB source codes for the optimization algorithms, i.e., Real-Coded GA, PSO, BBO, DE, and Firefly Algorithm, were taken from the yarpiz.com (http://yarpiz.com/ last accessed: August 2016). The parameters of the optimization algorithms used for the comparison purpose were taken in accordance with their original papers.

As seen from the entries the *Se*, *Sp*, *Acc*, *Auc*, and *Coeff* using the adaptive FKNN are larger than the traditional KNN when employing any of the algorithms at the parameter optimization stage. Moreover, the best results were attained using the PFree BAT algorithm at the attribute selection and the parameter optimization stage. The obtained average values for *Sp*, *Acc*, *Auc*, and *Coeff* were 100% each for the proposed approach that is higher than that equal to 98%, 98.95%, 99% and 98% obtained using the traditional KNN. Better results are accredited to the usage of the PFree Bat algorithm at both stages. The proposed variant of the BAT algorithm has increased the diversity of the search space via which optimal features were selected at the first stage and the best values of '*k*' and '*m*' i.e. (*k_opt* and *m_opt*) at the later stage.

Moreover, the results attained using the proposed approach are statistically better than the competing algorithms. For statistical verification paired *t*-test is used that compares the results produced by the proposed algorithm with other competing algorithms. The test assumes the null hypothesis that the accuracy of the two algorithms is the same, against the alternative that the accuracy of the proposed algorithm is higher than the comparison method. If the result of the *t*-test is 1, then it specifies the rejection of the null hypothesis at a 5% significance level and the acceptance of the alternate hypothesis. If the result is 0, then the null hypothesis cannot be rejected at 5% significance level. The last column of Table 2 reports the statistical significance level of the difference of accuracy value for the proposed algorithm w.r.t. to other meta-heuristic algorithms. For every pairwise comparison, a *p* value less than 0.05 was obtained. Typically, in contrast to the time-variant PSO, the *p* value was equal to 0.0035 signifying that accuracy for the proposed algorithm is significantly better than the competing optimized FKNN variant for every fold.

Table 3 summarizes the attained values of '*k_opt*' and '*m_opt*' for each value of the outer fold. The attained values for '*k_opt*' and '*m_opt*' at each fold were equal to 1, 2, 2, 2, 1 (values were rounded as they signify the nearest neighbors) and 0.4132, 1.7826, 0.9320, 1.9565 and 0.2134 using the proposed PFree Bat algorithm. At each fold of the data, the PFree Bat algorithm adaptively specifies these values. With this optimal combination of model parameters, i.e., '*k_opt*' and '*m_opt*'; FKNN obtained the best classification accuracy in each fold of data.

5.2 Performance evaluation of the proposed CAD with original extracted feature space (without feature selection)

The classification capability of PFree BAT Enhanced FKNN without feature selection is also investigated, and the findings are summarized in Table 4. The PFree Enhanced FKNN model operating on the complete extracted feature space reaches to an average *Se*, *Sp*, *Acc*, *Auc*, and *Coeff* values of 91.11%, 92%, 91.58%, 92.67%, and 85.74%. The obtained value of *k_opt*, and *m_opt* are 1,3,1,3,1 and 0.6481, 2.2786, 0.6497, 2, and 0.3820 respectively.

Table 3 Obtained values of k_opt and m_opt using various optimization algorithms for BRATS dataset

Method for feature selection	Algorithm used for the classifier parameter optimization	Folds	*k_opt*	*m_opt*
Fisher + RGA	RGA	1	2	2.2442
		2	4	1.2713
		3	2	2.2854
		4	2	1.1851
		5	5	3.8491
Fisher + PSO	PSO	1	4	1.2004
		2	1	2.4174
		3	1	2.9559
		4	5	2.5367
		5	5	2.2329
Fisher + BBO	BBO	1	1	0.6481
		2	3	2.2786
		3	1	0.6497
		4	3	2.0000
		5	1	0.3820
Fisher + Cuckoo Search [86, 87]	Cuckoo Search [86, 87]	1	2	1.2954
		2	2	1.0038
		3	2	1.0032
		4	3	1.853
		5	1	2.4257
Fisher + Firefly Algorithm [74]	Firefly Algorithm	1	5	1.7047
		2	3	1.4176
		3	5	3.2442
		4	3	1.4608
		5	3	2.2857
Fisher + Improved Harmony Search [54]	Harmony Search [54]	1	3	1.2723
		2	1	2.2670
		3	5	1.2953
		4	3	1.0975
		5	3	2.4969
Fisher + Bat Algorithm [84]	Bat Algorithm [84]	1	6	1.6418
		2	4	1.8443
		3	4	1.8811
		4	3	1.2936
		5	3	1.8707
Fisher + Novel Bat with Habitat Selection [57]	Novel Bat with Habitat Selection [57]	1	3	1.3070
		2	3	1.0313
		3	2	1.7373
		4	4	2.2349
		5	2	2.3278
Fisher + DE [10, 78]	DE [10, 78]	1	2	3.8418
		2	6	1.1544
		3	10	2.4533
		4	5	1.3706
		5	3	1.5620
Fisher + Time variant PSO [7]	Time variant PSO	1	1	1.0822
		2	3	0.9388
		3	2	0.9355
		4	3	1.0033
		5	2	1.0031
Fisher + PFree Bat Algorithm (Proposed)	PFree Bat Algorithm (Proposed)	2	1	0.4132
		3	2	1.7826
		4	2	0.932
		5	2	1.9565
		5	1	0.2314

k_opt: Optimal value for k-nearest neighbor;

m_opt: Optimal value of fuzzy strength parameter

RGA: Real Coded GA; PSO: Particle Swarm Optimization; BBO: Biogeography Based Optimization; DE: Differential Evolution; PFree BAT: Parameter Free BAT

Table 4 Results obtained by PFree BAT enhanced FKNN classifier without Feature Selection on BRATS dataset

Fold	*k_opt*	*m_opt*	*Se*	*Sp*	*Acc*	*Auc*	*Coeff*
1	1	0.6481	0.8889	0.8	0.8421	0.8444	0.6889
2	3	2.2786	1	1	1	1	1
3	1	0.6497	1	0.8	0.8947	0.9	0.809
4	3	2.0000	0.7778	1	0.8947	0.8889	0.8051
5	1	0.3820	0.8889	1	0.9474	0.9444	0.8989
Mean	1.8	1.1917 (0.7848)	0.9111	0.9200	**0.9158**	0.9156	0.8404
(SD)	(0.9798)		(0.0929)	(0.1095)	(0.0609)	(0.0482)	(0.1039)

Se: Sensitivity; *Sp*: Specificity; *Acc*: Accuracy; *Auc*: Area under the curve; *Coeff*: Mathew correlation coefficient; *k_opt*: Optimal value for k-nearest neighbor; *m_opt*: Optimal value of fuzzy strength parameter; SD: Standard Deviation

From the tabular findings it is concluded that with feature selection, the PFree BAT enhanced FKNN shows an improvement of 9.76%, 8.7%, 9.19%, 7.91% and 16.63% in *Se*, *Sp*, *Acc*, *Auc*, and *Coeff* in contrast to PFree BAT Enhanced FKNN working on the complete feature set. Moreover, this improvement is statistically significant (p value = 0.0017).

6 Discussions

This section is dedicated to the comparison of the proposed CAD with the existing state of the artworks. Firstly, the comparison is done with the works reported on brain tumor categorization. Secondly, the performance is contrasted with existing brain image classification schemes for Version 2 and 3 of the dataset from Harvard Medical Repository. Thirdly, performance comparison is done with existing classification schemes for PD dataset taken from the UCI Machine learning repository having a fixed set of the extracted feature space. Lastly, the validation is done on six benchmark datasets from KEEL repository having a fixed set of the extracted feature space solely to contrast the performance with existing FKNN variants.

6.1 Comparison with existing state-of-art works reported in the domain of brain tumor categorization

Table 5 compares the performance of the proposed CAD with the recent state of artworks dealing with the classification of the glioma images [4, 26, 27, 40, 67, 68, 72, 75, 81, 90, 93]. The proposed CAD outperformed the competing algorithms by achieving 100% *Se*, *Sp*, and *Acc*. Therefore, the proposed method is fully capable of detecting the glioma grade i.e. low or high than the other presented approaches which is highly desirable in clinical applications like therapy planning. This is entirely attributed to the designed CAD system incorporating the proposed PFree BAT enhanced FKNN classifier that has proven to be highly decisive for classification. As the works reported in [4, 26, 27, 40, 67, 68, 72, 75, 81, 90, 93], also deals with the glioma classification, the objective comparison is difficult to draw since the results have been obtained on their collected private datasets. However, for the method in [38] as the database was available from the Harvard Medical school, so the proposed approach has been duly validated on this dataset also. On this dataset also, the proposed approach yielded 100% *Sp* and *Acc* which is better than the average value equal to 99.18% and 97.95% reported in [38].

Table 5 Comparison with the similar works in the field of brain tumor classification

Reference	Total number of images and employed manner of ROI delineation	Features/Approach, Classifier and Partition scheme	Performance		
			Se	*Sp*	*Acc*
[40]	N^{total} = 26 (Glioblastoma multiform) **ROI delineation:** Region of contrast enhancement was manually contoured	**Features:** Attributes extracted from spectroscopic, diffusion and perfusion weighted images **Selection:** GA **No. of features**: 7 **Classifier:** k-NN **Partition Scheme:** LOOM	78	79	–
[90]	N^{total} = 102 brain tumors: Metastasis (24), Meningiomas (4), Gliomas grade 2 (22), Gliomas grade 3 (18), Glioblastomas (34) **ROI delineation:** 4 ROI's were manually traced	**Features:** i) shape and statistical features ii) Image intensity features iii) Gabor texture features which were extracted using 5 wavelengths and 8 orientations **Selection:** SVM with recursive feature elimination [23, 63] **No. of features:** 20 **Classifier:** SVM **Partition Scheme:** LOOM	Metastases vs. gliomas 87 HG vs. LG 85	79 96	85 88
[81]	N^{total} = 25 solitary metastases and 38 glioblastomas **ROI delineation:** Semiautomatic segmentation method based on the region intensity and standard deviation w.r.t the contralateral normal White matter	**Features:** Diffusion tensor imaging metrics **Selection:** NA **Classifier:** Logistic Regression **Partition Scheme:** NA	92	100	–
[27]	N^{total} = 65 metastases, 63 gliomas, 51 astrocytoma, and 71 meningioma images **ROI delineation:** No ROI delineation statistics were computed from the Gabor Filtered image	**Features:** Features from the DWT coefficients **Selection:** NA **No. of features**: 8 **Classifier:** Kohonen-Hopfield Neural Network **Partition Scheme:** Fixed Partition	–	–	93.60
[93]	N^{total} = 6 grade I, 32 grade II, 14 grade III, 49 grade IV **ROI delineation:** ROI's were extracted using un-supervised C-means Fuzzy clustering technique [17]	**Features:** Statistics derived from the image histogram **Selection:** PCA **No. of principal components**: 3 **Classifier:** SVM **Partition Scheme:** Ten-Fold Cross Validation	89	84	85
[67]	N^{total} = 428 images from 55 patients comprising of astrocytoma (AS), glioblastoma multiforme (GBM), childhood tumor-medulloblastoma (MED), meningioma (MEN), secondary tumor-metastatic (MET), and normal regions (NR) **ROI delineation:** Segmentation performed using CBAC [66]	**Features:** GLCM features, LOG features, RICGFs, IBFs, DGT features and RILBPs **No. of principal components:** 49 **Classifier:** ANN **Partition Scheme:** Ten-Fold cross-validation	–	–	91
[72]	N^{total} = 27 low-grade and 68 high-grade gliomas **ROI delineation:** Manual identification of the ROI	**Features:** Texture features at different anatomical scales varying from 2 mm to 6 mm **Selection**: NA	93	81	–

Table 5 (continued)

Reference	Total number of images and employed manner of ROI delineation	Features/Approach, Classifier and Partition scheme	Performance		
			Se	*Sp*	*Acc*
		Classification Type: Statistical Analysis **Partition Scheme:** NA			
[68]	N^{total} = 428 Images from 55 Patients (PGIMER database: D1) and 260 from SPL database (D2) **ROI delineation:** CBAC	**Features:** GLCM, LOG features, DGTFs features, RICGFs, RILBPFs, IBFs **Feature Selection/Reduction:** GA **No. of Features:** 71 **Classifier:** SVM, ANN **Partition Scheme:** LOOM	D1(GA-SVM, GA-ANN) 91.7, 94.9 D2 (GA-SVM, GA-ANN) 88, 94.1		
[75]	N^{total} = 200 T2-w images, 100 Low-Grade and 100 High-Grade **ROI delineation:** Fuzzy C Means Clustering, Edge based segmentation, and the watershed segmentation algorithm	**Features/FE Approach:** Shape, Intensity, and texture based features **Feature Selection/Reduction:** Shuffling Frog Leaping Algorithm/ **No. of Features:** 15 **Classifier:** SVM, LVQ and NB **Partition Scheme:** Random Partition (164: Training, 36: Testing)	(SVM, LVQ, NB) –	 –	 88.88, 91.67, 91
[38]	N^{total} = 30 healthy, 20 glioma **ROI delineation:** Classical Particle Swarm Optimization	**Features:** DSD + MSA **Feature Selection:** NA **Classifier:** SVM **No. of features:** 6 **Partition Scheme:** LOOM	100	94.78	98.01
[38]	N^{total} = 30 healthy, 20 glioma **ROI delineation:** Darwinian PSO	**Features:** DSD + MSA **Feature Selection:** NA **Classifier**: SVM No. of features: 6 **Partition Scheme:** LOOM	99.50	96.70	98.38
[38]	N^{total} = 30 healthy, 20 glioma **ROI delineation:** Fractional-order DPSO	**Features:** DSD + MSA **Feature Selection:** NA **No. of features:** 6 **Classifier:** SVM **Partition Scheme:** LOOM	100	97.95	99.18
[4]	N^{total} = 135 + 66 Images (67 H, 134 Ab) **ROI delineation:** Watershed, Fuzzy C Means (FCM), Discrete Cosine Transformation, and BWT	**Features:** First order Statistics, GLCM Features, and Tumor area **Feature Selection/Reduction:** GA **No. of Features:**11 **Classifier:** ANFIS, K-NN, and GA based classification **Partition Scheme:** NR	92.36	91.42	92.03
[26]		**Features/FE Approach:** Gray Level Difference method	96	98	98.1

Table 5 (continued)

Reference	Total number of images and employed manner of ROI delineation	Features/Approach, Classifier and Partition scheme	Performance		
			Se	*Sp*	*Acc*
	N^{total} = 450 T2-w images from four different abnormal categories such as metastase, glioma, astrocytoma and meningioma **ROI delineation:** No ROI delineation	**Feature Selection/Reduction:** Modified GA (Modifying the reproduction operators **No. of Features:** 9 **Classifier:** Back Propagation neural network **Partition Scheme:** Random (120: Training, 330: Testing)			
[22]	N^{total} = 120 HG, 80 LG (T1 and T1-CE): BRATS 2012 **ROI delineation:** Adaptive thresholding with Morphological operation	**Features:** Geometric Features including the area and parameter of tumor **Feature Selection/Reduction:** NA **No. of Features:** NR **Classifier:** Ensemble of SVM, KNN, and NB Classifier **Partition Scheme:** 10-fold CV	LG/HG 93/98.20	LG/HG 98.9/93.67	LG/HG 94.40/94
[22]	N^{total} = 120 HG, 80 LG (T2, FLAIR): BRATS 2012 **ROI delineation: Canny Edge detection and morphological operation**	**Features:** Geometric Features including the area and parameter of tumor **Feature Selection/Reduction:** NA **No. of Features:** NR **Classifier:** Ensemble of SVM, KNN, and NB Classifiers **Partition Scheme:** 10-fold CV	LG/HG 98.1/97.20	LG/HG 95.2/98.2	LG/HG 96.5/97
Proposed CAD	N^{total} = 60 Low and 60 high-grade glioma images from BRATS dataset **ROI delineation:** Fully automatic ROI delineation technique previously proposed by authors [34]	**Feature:** First-Order Statistics, GLCM, GLRM, GTDM, LTF, Fractal, Gabor Filters, Gabor Wavelet, and EMD based features **Selection:** Fisher + PFree Bat Algorithm [35] **No of features:** 1 **Classification:** Proposed PFree BAT enhanced FKNN classifier **Partition Scheme:** 5-Fold CV	**100**	**100**	**100**
Proposed CAD	N^{total} = 30 healthy, 20 glioma (Same dataset as used in [38]) (Version 1) **ROI delineation:** No ROI delineation needed	**Feature:** First-Order Statistics, GLCM, GLRM, GTDM, LTF, Fractal, Gabor Filters, Gabor Wavelet, and EMD based features **Selection:** Fisher + PFree Bat Algorithm [35] **No of features:** 1 **Classification:** Proposed PFree BAT enhanced FKNN classifier **Partition Scheme:** 5-Fold CV	**100**	**100**	**100**

-: Data not reported; *Se*: Sensitivity; *Sp*: Specificity; *Acc*: Accuracy; HG: high- Grade; LG: low-Grade; N^{total}: Total number of images; ROI: Region of interest; NR: Not Reported

GA: Genetic Algorithm

LOOM: Leave one out method

SVM: Support Vector Machine
DWT: Discrete Wavelet Transform
CBAC: Content-Based-Active Contour Model
PCA: Principal Component Analysis
ANN: Artificial Neural Network
GLCM: Gray level co-occurrence matrix
RICGFs: Rotation invariant circular Gabor features
LOG: Laplacian of Gaussian
LBP: Local binary patterns
DGT: Directional Gabor texture
RILBPFs: Rotation invariant local binary pattern features
IBF: Intensity based features (IBFs)
LVQ: Learning Vector Quantization
NB: Naive Bayes
DSD: Directional Spectral Distribution(DSD)
MSA: Multi-scale-analysis MSA
FCM: Fuzzy C Means
BWT: Berkley Wavelet Transform
ANFIS: Adaptive neurofuzzy inference system
KNN: K-Nearest Neighbor
GLRM: Gray Level Run Length Matrix
GTDM: Gray Tone Difference Matrix
LTF: Law's Texture Features
EMD: Empirical mode decomposition

Just for indication the works by [4, 26, 27, 68, 75, 90] dealing with the collected private tumor dataset, have reached to an *Acc* values equal to 88%, 93.60%, 94.9%, 91.67%, 92.03%, and 98.1%.

Although, not directly comparable the results for the CAD system employing the proposed PFree BAT enhanced FKNN model are better than the reported works in terms of the *Se*, *Sp*, and *Acc* that were 100% for the BRATS 2012 dataset. Recently, the work by [22] has addressed the tumor grade classification problem using BRATS 2012 dataset via the design of a CAD system consisting of phases of preprocessing, segmentation, feature extraction, and classification. The authors attained 94% and 97% accuracy (T1 and the FLAIR images) on a dataset comprising of 120 HG and 80 LG images. Our proposed work is comparable to [22] with the advantage that there was no need for any preprocessing stage of cropping and the image enhancement. The proposed CAD provides automatic classification without using any pre-processing on images.

Furthermore, the proposed CAD using PFree BAT enhanced FKNN model offers multiple benefits in contrast to similar works reported in this field as indicative from Table 5. First, it provides high accuracy not only for BRATS 2012 dataset but also for the dataset reported in the works by [38]. Second, the proposed PFree BAT enhanced FKNN classifier gives this performance using least number of features, i.e., just a single feature in contrast to existing works like [4, 26, 38, 40, 68, 90] that have utilized a feature space of 7, 20, 71, 6, 11, and 9 respectively for classifier training. Lastly, the proposed CAD does not involve any pre-processing stages of cropping and enhancement as reported in the existing work by [22].

6.2 Performance comparison with existing brain image classification schemes for version 2 and 3 of the dataset from Harvard medical repository [25]

Table 6 reports the performance comparison of the proposed CAD with the existing works on brain image classification using Version 2 and version 3 of the dataset from the Harvard Repository. From the Table 6, it is seen that most the works have employed the optimization techniques like PSO [91], ABC-PSO [82], BBO [88], and BAT [52] etc. for the tuning of the model parameters of the classifier.

From Table 6, it is inferred that the proposed CAD that employs the PFree BAT algorithm for FKNN parameter tuning have attained 100% accuracy for Version 2 and 3 of the dataset. It is superior to the value equal to 97.78%, 99.75%, 99.30%, 97.78%, 98.33%, and 99.75% obtained by the techniques devised in works by [52, 59, 82, 88, 91, 92]. Most of the approaches have attained 100% accuracy on the Version 2; their performance declines when moving over to bigger datasets [52, 59, 82, 88, 91, 92]. While few of the approaches given in Table 6 have reached to 100% accuracy both for Version 2 and 3 of the dataset like those presented in [60] but they use a feature count of 3. The prime advantage of the proposed CAD in contrast to [60] is that the proposed PFree enhanced FKNN classifier gives a ceiling value of the accuracy using just a single feature rather than employing a larger number of feature count.

6.3 Performance comparison with existing classification schemes for PD dataset taken from the UCI machine learning repository having a fixed set of the extracted feature space

To validate the versatility of the proposed PFree BAT enhanced FKNN algorithm on the fixed set extracted feature space, this section reports the results on the PD dataset from the UCI repository. For the fair comparison with existence works on the PD dataset, the results are computed without and with feature selection mechanism.

Table 6 Comparison with the similar works in the field of brain image classification using Version 2 and Version 3 from Harvard Repository

Reference	Image count and mechanism for ROI delineation	Features/Approach, Classifier and Partition scheme	Performance		
			Se	*Sp*	*Acc*
Zhang et al. [91]	N^{total} = 90 images (5 H, 85 Ab) **ROI delineation:** No ROI Delineation	**Features:** 2D-DWT (3 level decomposition using Haar wavelet) **Feature Selection:** PCA **Classifier:** PSO optimized Kernel SVM **Partition Scheme:** 5-Fold CV **No. of Features:** 1024 DWT coefficients	98.12	92	97.78
[82]	N^{total} = 66 Images (Version 2: 18 H, 48 Ab), 160 Images (Version 3: 20 H, 140 Ab) **ROI delineation:** No ROI delineation	**Features:** SWT **Feature Selection/Reduction:** PCA **Classifier:** IABAP-FNN **Partition Scheme:** 10 × 6-fold stratified CV (Version 2), 10 × 5-fold stratified CV (Version 3) **No. of Features:** 7	Version 2		100
			Version 3		99.44
[82]	N^{total} = 66 Images (Version 2: 18 H, 48 Ab), 160 Images (Version 3: 20 H, 140 Ab) **ROI delineation:** No ROI delineation	**Features:** SWT **Feature Selection/Reduction:** PCA **Classifier:** ABC- standard particle swarm optimization (SPSO)-FNN **Partition Scheme:** 10 × 6-fold stratified CV, 10 × 5-fold stratified CV (Version 3) **No. of Features:** 7	Version 2		100
			Version 3		99.75
[59]	N^{total} = 66 Images (Version 2: 18 H, 48 Ab) **ROI delineation:** No ROI delineation	**Features:** DWT **Feature Selection/Reduction:** PCA **Classifier:** ADBRF **Partition Scheme:** 5 × 6-fold stratified CV, 5 × 5-fold stratified CV **No. of Features:** 13	Version 2		
			–	–	100
			Version 3		
			–	–	99.30
[88]	N^{total} = 90 Images (5 H, 85 Ab) **ROI delineation:** No ROI delineation	**Features:** Wavelet Energy from the decomposed sub-bands **Feature Selection/Reduction:** NA **Classifier:** SVM with its weights optimized by the BBO Algorithm **Partition Scheme:**5 × 5 fold CV **No. of Features:** 10	98.12	92.00	97.78
[52]	N^{total} = 132 MR brain images (18 H, 114 Ab) **ROI delineation: No ROI delineation**	**Features:** Wavelet Entropy from the subbands decomposed using 2D Haar wavelet **Feature Selection/Reduction:** NA **Classifier:** BAT optimized ELM **Partition Scheme:** 10 × 10 fold CV **No. of Features:** 7	99.04	93.89	98.33
[60]	N^{total} = 66 Images (Version 2: 18 H, 48 Ab), 160 Images (Version 3: 20 H, 140 Ab) **ROI delineation:** No ROI delineation	**Features:** Ripplet-II Features **Feature Selection/Reduction:** PCA **Classifier:** Modified PSO based ELM **Partition Scheme:**6-Fold (Version 2), 5-Fold (Version 3) **No. of Features:** 13	**Version 2**		
			100	100	100
			Version 3		
			99.64	99.50	99.62
[60]	N^{total} = 66 Images (Version 2: 18 H, 48 Ab), 160 Images (Version 3: 20 H, 140 Ab) **ROI delineation:** No ROI delineation but requires preprocessing by CLAHE	**Features:** Ripplet-II Features **Feature Selection/Reduction:** PCA + LDA **Classifier:** Modified PSO based ELM **Partition Scheme:**6-Fold (Version 2), 5-Fold (Version 3) **No. of Features:** 3	**Version 2**		
			100	100	100
			Version 3		
			100	100	100
[92]	N^{total} = 66 Images (Version 2: 18 H, 48 Ab), 160 Images (Version 3: 20 H, 140 Ab)	**Features:** Pseudo Zernike Moment **Feature Selection/Reduction:** NA **Classifier:** Kernel SVM (RBF Kernel)	**Version2**		
			100	100	100
			Version3		
			99.93	98.50	99.75

Table 6 (continued)

Reference	Image count and mechanism for ROI delineation	Features/Approach, Classifier and Partition scheme	Performance		
			Se	*Sp*	*Acc*
	ROI delineation: No ROI Delineation	**Partition Scheme:** 10 × 6 Fold Stratified CV for Version 2, 10 × 5 Fold Stratified CV for Version 3 **No. of Features:** 400			
Proposed CAD	$\overline{N^{total}}$ = 66 Images (Version 2: 18 H, 48 Ab), 160 Images (Version 3: 20 H, 140 Ab) **ROI delineation:** No ROI delineation	**Feature:** First-Order Statistics, GLCM, GLRM, GTDM, LTF, Fractal, Gabor Filters, Gabor Wavelet, and EMD based features **Selection:** Fisher + PFree Bat Algorithm [35] **Classification:** Proposed PFree BAT enhanced FKNN classifier **Partition Scheme:** 5-Fold CV **No. of Features:** 1	**Version 2** **100** Version 3 100	**100** 100	**100** 100

-:Data not reported; *Se*: Sensitivity; *Sp*: Specificity; *Acc*: Accuracy; HG: high- Grade; LG: low-Grade; N^{total}: Total number of images; ROI: Region of interest; NR: Not Reported

DWT: Discrete Wavelet Transform

PCA: Principal Component Analysis

PSO: Particle swarm optimization

SVM: Support Vector Machine

CV: Cross-validation

SWT: Stationary wavelet transform

IABAP-FNN: Integrated algorithm based on artificial bee colony (ABC) and particle swarm optimization (IABAP)-Feed Forward Neural Network (FNN)

ADBRF: AdaBoost with random forests (ADBRF)

BBO: Biogeography based optimization

ELM: Extreme Learning Machine

GLCM: Gray level co-occurrence matrix

GLRM: Gray Level Run Length Matrix

GTDM: Gray Tone Difference Matrix

LTF: Law's Texture Features

EMD: Empirical mode decomposition

6.3.1 Classification using the proposed PFree BAT enhanced FKNN model with whole original feature space

In this experiment, we evaluated the effectiveness of PFree BAT enhanced FKNN model on the original feature space. The detailed results attained by the PFree BAT enhanced FKNN classifier are shown in Table 7. From, the Table 7, it is seen that PFree BAT enhanced FKNN classifier had reached to average *Se*, *Sp*, *Acc*, *Auc*, and *Coeff* values equal to 97.24%, 98%, 97.45%, 97.63%, and 93.58%. The attained values are better than the works reported in [9] in which they obtained the values equal to 96.93%, 88.78%, 94.63%, and 92.85% for *Se*, *Sp*, *Acc*, and *Auc*.

In addition, it is seen from the Table 7 that the value of the *k_opt* and *m_opt* are adaptively specified by PFree BAT optimization algorithm for each run which is the probable reason that the proposed adaptive FKNN classifier performed better than [9].

Table 7 Results obtained by PFree BAT enhanced FKNN classifier without Feature Selection on Parkinson Dataset

Fold	*k_opt*	*m_opt*	*Se*	*Sp*	*Acc*	*Auc*	*Coeff*
1	3	1.2542	1	1	1	1	1
2	6	1.5333	1	1	1	1	1
3	6	1.2546	0.9667	1	0.9744	0.9833	0.9327
4	3	1.2809	0.931	1	0.9487	0.9655	0.8808
5	7	1.4045	0.9655	0.9	0.9487	0.9328	0.8655
Mean	5	1.3455	**0.9724**	**0.9800**	**0.9745**	0.9763	0.9358
(SD)	(1.5275)	(0.0996)	(0.0476)	(0.0632)	(0.0358)	(0.0230)	(0.0519)

Se: Sensitivity; *Sp*: Specificity; *Acc*: Accuracy; *Auc*: Area under the curve; *Coeff*: Mathew correlation coefficient; *k_opt*: Optimal value for k-nearest neighbor; *m_opt*: Optimal value of fuzzy strength parameter; SD: Standard Deviation

6.3.2 Classification using the proposed PFree BAT enhanced FKNN model with feature selection

In order to investigate whether feature selection can further improve the detection performance for PD, the PFree BAT enhanced FKNN model was applied to the reduced feature space. Fisher criterion was used in conjunction to rank the features [35]. The top 1, 5, 10, 15, and 20 features are given in Table 8. Table 9 lists the detailed results of PFree BAT enhanced FKNN in terms of *Se*, *Sp*, *Acc*, *Auc*, and *Coeff*. From Table 9, it is seen that the performance of the PFree BAT enhanced FKNN model built with feature subset size of 15 is better than one built with all the features. Typically for a feature count equal to 15 the achieved average *Se*, *Sp*, *Acc, Auc,* and *Coeff* were equal to 97.33%, 100%, 98%, 98.60%, and 97.30% which is higher than the comparison algorithms presented in [9] that reported a mean value of 97.27%, 91.11%, 95.49%, and 94.19% for *Se*, *Sp*, *Acc, Auc,* and *Coeff*. At each feature count (1, 5, 10, 15, 20, 22) the obtained *Se*, *Sp*, *Acc* and *Auc* attained via the adaptive FKNN is much higher than the comparison works reported in the literature [9]. Moreover, from the tabular results it is seen that with the utility of the feature selection, the PFree enhanced FKNN has improved performance. The *Se*, *Sp*, *Acc*, *Auc*, and *Coeff* measures improvise by 0.09%, 2.04%, 0.56%, 1.74% and 2.1% in contrast to without feature selection. Moreover, this improvement is statistically significant (p value = 0.0429).

The optimal value of '***k***' and '***m***' obtained via the PFree enhanced FKNN classifier working on the reduced feature space, i.e., for a typical feature count of 15, at each subsequent fold are given in Table 10. The increase in the value of the performance metrics is attributed to the generation of '***k_opt***', and '***m_opt***' by the application of the PFree BAT enhanced FKNN classifier on the reduced dataset.

Table 8 Optimal feature subset obtained by the proposed technique

Count	Optimal Feature subset
1	F22
5	F22 F17 F8 F19 F1
10	F20 F1 F18 F21 F11 F17 F22 F14 F4 F15
15	F22 F17 F7 F18 F6 F19 F14 F20 F10 F1 F4 F13 F12 F16 F5
20	F22 F3 F4 F13 F18 F12 F7 F1 F16 F10 F15 F14 F20 F5 F21 F6 F2 F17 F11 F8

Table 9 Performance of the proposed technique using different set of optimal features

Feature subset	*Se* [9]	*Sp* [9]	*Acc* [9]	*Auc* [9]	*Coeff* [9]	*Se* (Proposed)	*Sp* (Proposed)	*Acc* (Proposed)	*Auc* (Proposed)	*Coeff* (Proposed)
1	0.9320 (0.0021)	0.6059 (0.0368)	0.8562 (0.0017)	0.7689 (0.0188)	–	**0.9660** (0.0218)	0.6022 (0.1039)	**0.8769** (0.0251)	**0.8084 (0.1037)**	**0.6631 (0.2042)**
5	0.9571 (0.0087)	0.7301 (0.0235)	0.8988 (0.0087)	0.8436 (0.0151)	–	**0.9726** (0.0288)	**0.7933** (0.1206)	**0.9282** (0.0280)	**0.8785** (0.0358)	**0.7864** (0.0523)
10	0.9679 (0.0077)	0.8012 (0.0426)	0.9283 (0.0114)	0.8845 (0.0226)	–	**0.9724** (0.0450)	**0.9156** (0.0918)	**0.9589** (0.0429)	**0.9541** (0.0209)	**0.9067** (0.0364)
15	0.9727 (0.0067)	0.9111 (0.0274)	0.9549 (0.0061)	0.9419 (0.0141)	–	**0.9733** (0.0344)	**1** (0)	**0.9800** (0.0262)	**0.9866** (0.0194)	**0.9730** (0.0329)
20	0.9761 (0.0076)	0.9112 (0.0140)	0.9597 (0.0050)	0.9437 (0.0076)	–	0.9593 (0.0284)	**1** (0)	**0.9692** (0.0215)	**0.9797** (0.0142)	**0.9249** (0.0510)
All Features	0.9693 (0.0058)	0.8878 (0.0317)	0.9463 (0.0075)	0.9285 (0.0153)	–	**0.9724** (0.0476)	**0.9800** (0.0632)	**0.9745** (0.0358)	**0.9763** (0.0230)	**0.9358** (0.0519)

Se: Sensitivity; *Sp*: Specificity; *Acc*: Accuracy; *Auc*: Area under the curve; *Coeff*: Mathew correlation coefficient

Table 10 Results obtained by PFree BAT enhanced FKNN classifier with Feature Selection on Parkinson Dataset

Fold	*k_opt*	*m_opt*	*Se*	*Sp*	*Acc*	*Auc*	*Coeff*
1	5	1.2885	1	1	1	1	1
2	3	1.6542	1	1	1	1	1
3	1	1	0.9667	1	0.9743	0.9833	0.9327
4	4	1.111	1	1	1	1	1
5	7	1.0978	1	0.9	0.97435	0.95	0.9327
Mean(SD)	4	1.2303	**0.9733**	**1**	**0.9800**	**0.9866**	**0.9730**
	(1.8257)	(0.2113)	(0.0344)	(0)	(0.0262)	(0.0194)	(0.0329)

Se: Sensitivity; *Sp*: Specificity; *Acc*: Accuracy; *Auc*: Area under the curve; *Coeff*: Mathew correlation coefficient; *k_opt*: Optimal value for k-nearest neighbor; *m_opt*: Optimal value of fuzzy strength parameter; SD: Standard Deviation

For the sake of comparison, the classification accuracies attained by the existing approaches on the benchmark PD dataset are given in Table 11. As indicated in the table, accuracy rates ranging between 74% and 96% have been achieved by the other existing works. The proposed approach surpasses the competing algorithms by achieving the mean value of accuracy as 98% and the best value as 100% at a feature count of 15. The increase has been equal to 2% in the average accuracy and 4% in the best accuracy value with feature selection in contrast to the existing work in [9]. Moreover, in contrast to [6], the increase has been 0.8% via the proposed PFree BAT enhanced FKNN classifier using all the 22 features.

6.4 Performance comparison with existing FKNN variants for the six benchmark datasets from KEEL repository having a fixed set of the extracted feature space

This section compares the proficiency of the proposed PFree BAT enhanced FKNN system over six benchmark datasets from KEEL repository. This dataset has been specially chosen to compare the performance of the proposed technique with other FKNN variants as reported in the works by Derrac et al. [16]. Just for the comparative purpose, the results have been reported under the same test conditions as given in [16]. Three sets of test conditions were taken as given below, and the *Acc* was computed as given in Table 12

1. Fixed k and optimized m
2. Fixed k, optimized m, and Feature Selection
3. Optimized k, optimized m, and Feature Selection

The results under the three test conditions show how the uncertainty in the selection of the k value is reduced by the optimization algorithm and the feature selection process through which an increase in the average accuracy was achieved.

The results are supplemented by the nonparametric statistical tests, i.e., Friedman Shaffer with the post-hoc procedure. The best results for *Acc* were obtained for the third test condition followed by second and first.

The results presented in this section indicate that the proposed method is scalable to classification problems having a larger sample size and varying dimensionality. The proposed method is validated on eleven benchmark datasets with the sample size varying from 66 to 569, and feature space varying from 6 to 52. The attained accuracy values for most of these

Table 11 A comparative analysis of the classification accuracy achieved using the proposed and other competing techniques

Ref	Technique	Training Scheme	*Acc* (%)
[49]	Pre-selection filter +exhaustive search + SVM	Bootstrap with 50 replicates	91.4
[14]	ANN	Hold-out	92.9
[3]	Parallel Feed-Forward Neural Network	Hold-out	91.20
[69]	Mutual information based feature selection +SVM	Bootstrap with 50 replicates	92.75
[48]	Fuzzy-based non-linear transformation +SVM	Hold-out	93.47
[70]	Dirichlet process mixtures	5-fold CV	87.7
[62]	Improved- multiclass multi-kernel relevance vector machines (mRVMs)	10-fold CV	89.47
[21]	Genetic-Programming & Expectation Maximization Algorithm	10-fold CV	93.1
[53]	Fuzzy entropy measures + Similarity classifier	Hold-out	85.03
[61]	Correlation Based Feature Selection (CFS) Algorithm with RF ensemble classifier	10-fold CV	87.1
[73]	Particle Swarm Optimization + Optimum Path Forest (OPF)	Hold-out	73.53
[73]	Harmony Search + OPF	Hold-out	84.01
[73]	Gravitational search algorithm + OPF	Hold-out	84.01
[8]	Principle component analysis + Fuzzy – KNN (FKNN)	10-fold CV outer loop+5-fold CV on inner loop	96.07
[39]	Neural Network with weighted fuzzy membership(WFM) function employing bounded sum of WFM	5-fold CV	88.2 (4 Features) 86.2 (22 Features)
[9]	Maximum relevance minimum redundancy + Kernelized version of extreme learning machine (mRMR-KELM)	10-fold CV outer loop+10-fold CV on inner loop	95.97 96.47 (Best)
[71]	Binary Bat Algorithm (BBA) + Feed forward back propagation based network	_	93.60 (6 Features)
[6]	Chaotic Bacterial Foraging Optimization Enhanced Fuzzy KNN Approach	10-fold CV	96.97 (22 features)
Proposed Technique	**Proposed Algorithm (Fisher + PFree Bat (Feature Selection)) + PFree Bat enhanced FKNN classifier**	5-fold CV outer loop +3-fold CV on inner loop	**97.45 (22 Features)** **94.59 (6 Features)** **98.00 (mean at 15 features)** **100 (Best value: 15 features)**

Table 12 Analysis of the proposed PFree enhanced FKNN classifiers for different datasets at k = 3,5,7, and 9

Methods	Dataset							
	Appendictis	Bupa	Heart	Hepatitis	Monk-2	Wdbc	Friedman Rank Value	Holm *p* value
K = 3								
M1	84.18	61.19	79.26	82.51	84.33	96.65	5.25	**0.0311**
M2	84.27	60.66	77.41	82.51	96.29	96.48	6.3333	0.0631
M3	87	60.27	80.74	82.51	78.33	96.3	6	0.0569
M4	84.27	60.95	77.41	82.51	96.29	96.48	6	0.0569
M5	87.91	59.73	79.26	82.51	96.29	96.31	5.5	**0.0403**
M6	87.91	62.04	79.26	82.69	79.77	96.65	3.5833	**0.0013**
M7	87	62.67	79.63	82.51	79.47	96.48	4.6667	**0.0135**
M8	84.27	60.9	78.52	81.99	81.8	96.65	6.4167	0.0637
M9	82.36	59.99	78.52	80.26	72.52	95.43	9.4167	**0.0013**
M10	86.75	66.67	80.37	87.5	96.79	97.01	1.8333	
M11	87	67.54	82.22	87.73	96.79	97.19		
K = 5								
M1	86	65.44	79.63	86.51	91.97	97.18	4.6667	**0.0442**
M2	85.91	61.31	80.74	86.27	94.75	96.83	5.1667	**0.0233**
M3	87.91	62.5	80.37	83.42	89.69	96.65	6	**0.0067**
M4	85.91	61.31	80.74	86.27	94.75	96.83	5.1667	**0.0233**
M5	87.91	60.78	80	86.27	94.52	97.01	5.1667	**0.0233**
M6	87.82	61.11	78.52	85.02	81.82	96.83	7.5833	**0.0003**
M7	87.91	64.01	80.37	83.42	84.84	96.65	6	**0.0067**
M8	86.09	61.68	78.52	83.42	92.42	96.48	7.5	**0.0004**
M9	87.91	62.51	80	83.42	86.01	96.3	6.75	**0.0018**
M10	88.7	65.51	81.85	87.5	95.5	97.36	1	
M11	88.7	66.67	82.22	87.5	96.59	97.54		
K = 7								
M1	87.91	65.75	80	85.08	86.16	96.83	4.8333	**0.036**
M2	87.91	62.53	79.26	89.19	89.16	97.18	4.75	**0.04**
M3	87.91	63.13	79.63	85.08	84.11	97.01	5.6667	**0.0113**
M4	87.91	62.53	79.26	89.19	89.16	97.18	4.75	**0.04**
M5	87.82	62.26	78.15	89.19	87.34	97.01	7	**0.0011**
M6	87.91	61.67	79.63	82.36	80.17	96.3	8.0833	**0.0001**
M7	87.91	65.21	78.52	84.67	82.5	97.18	6.25	**0.0044**
M8	87.91	62.86	78.15	84.32	84.33	96.3	7.5833	**0.0003**
M9	87.91	65.17	79.26	86.09	82.97	97.36	5.0833	**0.0261**

Table 12 (continued)

Methods	Dataset							
	Appendictis	Bupa	Heart	Hepatitis	Monk-2	Wdbc	Friedman Rank Value	Holm p value
M10	88.74	67.54	82.22	90	89.81	97.37	1	
M11	88.74	68.11	82.59	91.25	94.19	97.54		
K = 9								
M1	86	65.13	79.26	82.66	85.78	96.65	7.9167	**0.0002**
M2	87.91	62.44	80.37	83.61	86.2	96.83	5.25	**0.0261**
M3	87.91	66.06	80.74	83.42	82.76	96.83	5	**0.036**
M4	87.91	62.44	80.37	83.61	86.2	96.83	5.25	**0.0261**
M5	86	61.9	80.74	84.61	86.2	96.83	5.6667	**0.0145**
M6	86.91	62.88	79.26	82.18	79.45	96.65	8.6667	**0.0001**
M7	87.91	66.92	80	84.32	81.39	97.18	4.3333	0.0773
M8	86.09	65.57	77.41	83	83.21	97.01	6.6667	**0.0028**
M9	87	65.4	80.74	83.59	81.87	97.18	5.0833	**0.0324**
M10	88.74	66.67	82.59	91.25	87.73	97.36	1.1667	
M11	88.74	67.54	82.59	92.5	91.9	97.36		
M12	**88.77**	**68.11**	**83.33**	**92.5**	**96.79**	**97.54**		

M1: EF-KNN [16]: Evolutionary FKNN

M2: KNN [13]

M3: Fuzzy-KNN [36]

M4: D-SKNN [15]: KNN based on Dempster –Shafer Theory

M5: IF-KNN [37]: Intuitionistic FKNN

M6: FENN [85]: Edited FKNN

M7: IT2FKNN [65]: Interval Type 2 FKNN

M8: GA Fuzzy-KNN [30]

M9: PFKNN [2]: Pruned FKNN

M10: Proposed method (k fixed, m optimized)

M11: Proposed method with Feature Selection (k-fixed m optimized)

M12: Proposed method with Feature Selection and optimized k and m

datasets were in the range from 88 to 100%. Moreover, the average run time for the datasets is in seconds. Just for indication, for the Parkinson dataset, using all the features the time taken by the PFree BAT enhanced FKNN classifier is 2 s and for tumor dataset, it is 3.54 s. Accuracy and the runtime value on different datasets with varying sizes and dimensionality are indicative that the PFree enhanced FKNN model is scalable in handling an increasing amount of data with larger feature space with minimum computation cost.

Future works will be focused on applying the proposed CAD for the task of the face and palmprint recognition [41–46]. Moreover, some advance feature extraction, feature selection, and learning methods like those presented in [47, 51] will be explored.

7 Conclusion

In this work, an automatic brain tumor diagnosis system has been developed. The core component of the system is the adaptive FKNN classifier whose maximum potential is explored by the PFree-BAT optimization algorithm resulting in the generation of the optimal value of neighborhood size and fuzzy strength parameter. Better classification accuracy obtained on the brain tumor dataset has proven that the proposed system can distinguish well enough between the patients with the different grades of glioma, i.e., Low-grade and High-grade and also healthy groups from the glioma patients. It was observed that PFree-Bat enhanced FKNN classifier while working on the reduced feature set achieved 100% recognition rate via fivefold cross-validation. Additionally, the versatility of the method was also proven by experimenting on the standard MR brain image dataset, Parkinson data set and the KEEL data sets. The promising results of the proposed method have shown that our designed system is also capable of distinguishing abnormal subjects from healthy groups. Extensive experimentation on benchmark data sets from KEEL repository also validates that the proposed mechanism is superior to the existing FKNN variants existing in the literature.

Funding This research received no specific grant from any funding agency in the public, commercial, or not-for-profit sectors.

Compliance with ethical standards

Conflict of interest 'None Declared'.

References

1. Amadasun M, King R (1989) Texural features corresponding to textural properties. IEEE Trans Syst Man Cybern 19:1264–1274
2. Arif M, Akram MU, others (2010) Pruned fuzzy K-nearest neighbor classifier for beat classification. J Biomed Sci Eng 3:380.
3. Astrom F, Koker R (2011) A parallel neural network approach to prediction of Parkinson's disease. Expert Syst Appl 38:12470–12474
4. Bahadure NB, Ray AK, Thethi HP (2018) Comparative approach of MRI-based brain tumor segmentation and classification using genetic algorithm. J Digit Imaging 31:477–489
5. Bakwad KM, Pattnaik SSSS, Sohi BS, et al (2009) Hybrid bacterial foraging with parameter free PSO. In: Nat. Biol. Inspired Comput. 2009. NaBIC 2009. World Congr. Ieee, pp 1077–1081
6. Cai Z, Gu J, Wen C et al (2018) An intelligent Parkinson's disease diagnostic system based on a chaotic bacterial foraging optimization enhanced fuzzy KNN approach. Comput Math Methods Med 2018:1–24

7. Chen H-L, Yang B, Wang G et al (2011) A novel bankruptcy prediction model based on an adaptive fuzzy k-nearest neighbor method. Knowledge-Based Syst 24:1348–1359
8. Chen H-L, Huang C-C, Yu X-G et al (2013) An efficient diagnosis system for detection of Parkinson's disease using fuzzy k-nearest neighbor approach. Expert Syst Appl 40:263–271
9. Chen H-L, Wang G, Ma C et al (2016) An efficient hybrid kernel extreme learning machine approach for early diagnosis of Parkinson′s disease. Neurocomputing 184:131–144
10. Cheng M, Hoang N (2014) Groutability estimation of grouting processes with microfine cements using an evolutionary instance-based learning approach. J Comput Civ Eng 28:04014014
11. Colominas MA, Schlotthauer G, Torres ME (2014) Improved complete ensemble EMD: a suitable tool for biomedical signal processing. Biomed Sign Proc Control 14:19–29
12. Costa AF, Humpire-mamani G, Juci A, et al (2012) An Efficient Algorithm for Fractal Analysis of Textures. In: 25th SIBGRAPI Conf. Graph. Patterns Images. IEEE, Ouro Preto, Brazil, pp 39–46
13. Cover T, Hart P (1967) Nearest neighbor pattern classification. IEEE Trans Inf Theory 13:21–27
14. Das R (2010) A comparison of multiple classification methods for diagnosis of Parkinson disease. Expert Syst Appl 37:1568–1572
15. Denoeux T (1995) A k-nearest neighbor classification rule based on Dempster-Shafer theory. IEEE Trans Syst Man Cybern 25:804–813
16. Derrac J, Chiclana F, García S, Herrera F (2016) Evolutionary fuzzy k -nearest neighbors algorithm using interval-valued fuzzy sets. Inf Sci (Ny) 329:144–163
17. Emblem KE, Nedregaard B, Hald JK et al (2009) Automatic glioma characterization from dynamic susceptibility contrast imaging: brain tumor segmentation using knowledge-based fuzzy clustering. J Magn Reson Imaging 30:1–10
18. Fawcett T (2004) ROC graphs: notes and practical considerations for researchers. Mach Learn 31:1–38
19. Georgiadis P, Cavouras D, Kalatzis I et al (2008) Improving brain tumor characterization on MRI by probabilistic neural networks and non-linear transformation of textural features. Comput Methods Prog Biomed 89:24–32
20. Gibbs P, Turnbull LW (2003) Textural analysis of contrast-enhanced MR images of the breast. Magn Reson Med 50:92–98
21. Guo P-F, Bhattacharya P, Kharma N (2010) Advances in detecting Parkinson's disease. In: Int. Conf. Med. Biometrics. pp 306–314
22. Gupta N, Bhatele P, Khanna P (2019) Glioma detection on brain MRIs using texture and morphological features with ensemble learning. Biomed Sign Proc Control 47:115–125
23. Guyon I, Weston J, Barnhill S, Vapnik V (2002) Gene selection for cancer classification using support vector machines. Mach Learn 46:389–422
24. Haralick RM, Shanmugam K, Dinstein I (1973) Textural features for image classification. IEEE Trans Syst Man Cybern SMC-3:610–621
25. Harvard Medical School. http://med.harvard.edu/AANLIB/. Accessed 2 Apr 2016
26. Hemanth JD, Anitha J (2019) Modified genetic algorithm approaches for classification. Appl Soft Comput J 75:21–28
27. Hemanth DJ, Vijila CKS, Selvakumar AI, Anitha J (2011) Performance Enhanced Hybrid Kohonen-Hopfield Neural Network for Abnormal Brain Image Classification. In: Signal Process. Image Process. Pattern Recognit. Springer, pp 356–365
28. Herlidou-Meme S, Constans J, Carsin B et al (2003) MRI texture analysis on texture test objects, normal brain and intracranial tumors. Magn Reson Imaging 21:989–993
29. Hong L, Wan Y, Jain A (1998) Fingerprint image enhancement: algorithm and performance evaluation. IEEE Trans Pattern Anal Mach Intell 20:777–789
30. Hu X, Xie C (2005) Improving fuzzy k-NN by using genetic algorithm. J Comput Inf Syst 1:203–213
31. Hui LY, Muftah M, Das T et al (2012) Classification of MR tumor images based on Gabor wavelet analysis. J Med Biol Eng 32:22–28
32. Iftekharuddin KM, Zheng J, Islam MA, Ogg RJ (2009) Fractal-based brain tumor detection in multimodal MRI. Appl Math Comput 207:23–41
33. Kaur T, Saini B, Gupta S (2017) Quantitative metric for MR brain tumor grade classification using sample space density measure of analytic intrinsic mode function representation. IET Image Process 11:620–632
34. Kaur T, Saini BS, Gupta S (2018) A joint intensity and edge magnitude-based multilevel thresholding algorithm for the automatic segmentation of pathological MR brain images. Neural Comput Appl 30:1317–1340
35. Kaur T, Saini BS, Gupta S (2018) A novel feature selection method for brain tumor MR image classification based on the fisher criterion and parameter-free bat optimization. Neural Comput Appl 29:193–206
36. Keller JM, Gray MR (1985) A fuzzy K-nearest neighbor algorithm. IEEE Trans Syst Man Cybern SMC-15: 580–585

37. Kucnehva LI (1995) An intuitionistic fuzzy k-nearest neighbors rule.
38. Lahmiri S (2017) Glioma detection based on multi-fractal features of segmented brain MRI by particle swarm optimization techniques. Biomed Sign Proc Control 31:148–155
39. Lee S-H (2015) Feature selection based on the center of gravity of BSWFMs using NEWFM. Eng Appl Artif Intell 45:482–487
40. Lee MC, Nelson SJ (2008) Supervised pattern recognition for the prediction of contrast-enhancement appearance in brain tumors from multivariate magnetic resonance imaging and spectroscopy. Artif Intell Med 43:61–74
41. Leng L, Zhang J, Xu J, et al (2010) Dynamic weighted discrimination power analysis in DCT domain for face and palmprint recognition. In: Inf. Commun. Technol. Converg. (ICTC), 2010 Int. Conf. pp 467–471
42. Leng L, Zhang J, Xu J, et al (2010) Dynamic weighted discrimination power analysis: A novel approach for face and palmprint recognition in DCT domain. In: Int. J. Phys. Sci. pp 467–471
43. Leng L, Zhang J, Chen G, et al (2011) Two-directional two-dimensional random projection and its variations for face and palmprint recognition. In: Int. Conf. Comput. Sci. Its Appl. pp 458–470
44. Leng L, Zhang S, Bi X, Khan MK (2012) Two-dimensional cancelable biometric scheme. In: 2012 Int. Conf. Wavelet Anal. Pattern Recognit. pp 164–169
45. Leng L, Li M, Teoh ABJ 2013) Conjugate 2D palmhash code for secure palm-print-vein verification. In: Image Signal Process. (CISP), 2013 6th Int. Congr. pp 1705–1710
46. Leng L, Li M, Kim C, Bi X (2017) Dual-source discrimination power analysis for multi-instance contactless palmprint recognition. Multimed Tools Appl 76:333–354
47. Li Z, Tang J (2015) Unsupervised feature selection via nonnegative spectral analysis and redundancy control. IEEE Trans Image Process 24:5343–5355
48. Li D-C, Liu C-W, Hu SC (2011) A fuzzy-based data transformation for feature extraction to increase classification performance with small medical data sets. Artif Intell Med 52:45–52
49. Little MA, McSharry PE, Hunter EJ et al (2009) Suitability of dysphonia measurements for telemonitoring of Parkinson's disease. IEEE Trans Biomed Eng 56:1015–1022
50. Liu DY, Chen HL, Yang B et al (2012) Design of an enhanced fuzzy k-nearest neighbor classifier based computer aided diagnostic system for thyroid disease. J Med Syst 36:3243–3254
51. Liu Y, Nie L, Han L, et al (2015) Action2Activity: Recognizing Complex Activities from Sensor Data. In: IJCAI. pp 1617–1623
52. Lu S, Qiu X, Shi J et al (2017) A pathological brain detection system based on extreme learning machine optimized by bat algorithm. CNS Neurol Disord Targets (Formerly Curr Drug Targets-CNS Neurol Disord) 16:23–29
53. Luukka P (2011) Feature selection using fuzzy entropy measures with similarity classifier. Expert Syst Appl 38:4600–4607
54. Mahdavi M, Fesanghary M, Damangir E (2007) An improved harmony search algorithm for solving optimization problems. Appl Math Comput 188:1567–1579
55. Mahmoud-Ghoneim D, Toussaint G, Constans J-M, de Certaines JD (2003) Three dimensional texture analysis in MRI: a preliminary evaluation in gliomas. Magn Reson Imaging 21:983–987
56. Materka A, Strzelecki M (1998) Texture analysis methods–a review. Tech. Univ. lodz, Inst. Electron. COST B11 report, Brussels
57. Meng X-B, Gao XZ, Liu Y, Zhang H (2015) A novel bat algorithm with habitat selection and Doppler effect in echoes for optimization. Expert Syst Appl 42:6350–6364
58. Menze BH, Jakab A, Bauer S et al (2014) The multimodal brain tumor image segmentation benchmark (BRATS). IEEE Trans Med Imaging 34:1993–2024
59. Nayak DR, Dash R, Majhi B et al (2016) Brain MR image classification using two-dimensional discrete wavelet transform and AdaBoost with random forests. Neurocomputing 177:188–197
60. Nayak DR, Dash R, Majhi B (2018) Discrete ripplet-II transform and modified PSO based improved evolutionary extreme learning machine for pathological brain detection. Neurocomputing 282:232–247
61. Ozcift A, Gulten A (2011) Classifier ensemble construction with rotation forest to improve medical diagnosis performance of machine learning algorithms. Comput Methods Prog Biomed 104:443–451
62. Psorakis I, Damoulas T, Girolami MA (2010) Multiclass relevance vector machines: sparsity and accuracy. IEEE Trans Neural Netw 21:1588–1598
63. Rakotomamonjy A (2003) Variable selection using SVM-based criteria. J Mach Learn Res 3:1357–1370
64. Ramana Murthy G, Senthil Arumugam M, Loo CK (2009) Hybrid particle swarm optimization algorithm with fine tuning operators. Int J Bio-Inspired Comput 1:14–31
65. Rhee F-H, Hwang C (2003) An interval type-2 fuzzy K-nearest neighbor. In: fuzzy Syst. 2003. FUZZ'03. 12th IEEE Int. Conf. Pp 802–807
66. Sachdeva J, Kumar V, Gupta I et al (2012) A novel content-based active contour model for brain tumor segmentation. Magn Reson Imaging 30:694–715

67. Sachdeva J, Kumar V, Gupta I et al (2013) Segmentation, feature extraction, and multiclass brain tumor classification. J Digit Imaging 26:1141–1150
68. Sachdeva J, Kumar V, Gupta I et al (2016) A package-SFERCB-"segmentation, feature extraction, reduction and classification analysis by both SVM and ANN for brain tumors". Appl Soft Comput 47:151–167
69. Sakar CO, Kursun O (2010) Telediagnosis of Parkinson's disease using measurements of dysphonia. J Med Syst 34:591–599
70. Shahbaba B, Neal R (2009) Nonlinear models using Dirichlet process mixtures. J Mach Learn Res 10: 1829–1850
71. Shrivastava P, Shukla A, Vepakomma P et al (2017) A survey of nature-inspired algorithms for feature selection to identify Parkinson's disease. Comput Methods Prog Biomed 139:171–179
72. Skogen K, Schulz A, Dormagen JB et al (2016) Diagnostic performance of texture analysis on MRI in grading cerebral gliomas. Eur J Radiol 85:824–829
73. Spadoto AA, Guido RC, Carnevali FL, et al (2011) Improving Parkinson's disease identification through evolutionary-based feature selection. In: 2011 Annu. Int. Conf. IEEE Eng. Med. Biol. Soc. pp 7857–7860
74. Subashini MM, Sahoo SK, Sunil V, Easwaran S (2016) A non-invasive methodology for the grade identification of astrocytoma using image processing and artificial intelligence techniques. Expert Syst Appl 43:186–196
75. Subashini MM, Sahoo SK, Sunil V, Easwaran S (2016) A non-invasive methodology for the grade identification of astrocytoma using image processing and artificial intelligence techniques. Expert Syst Appl 43:186–196
76. Tang X (1998) Texture information in run-length matrices. IEEE Trans Image Process 7:1602–1609
77. Tencer L, Reznakova M, Cheriet M (2012) A new framework for online sketch-based image retrieval in web environment. In: Inf. Sci. Signal Process. their Appl. Spec. Sess. IEEE, Montreal, QC, pp 1430–1431
78. Tien Bui D, Nguyen QP, Hoang ND, Klempe H (2016) A novel fuzzy K-nearest neighbor inference model with differential evolution for spatial prediction of rainfall-induced shallow landslides in a tropical hilly area using GIS. Landslides 14:1–17
79. Vidya KS, Ng EY, Acharya UR et al (2015) Computer-aided diagnosis of myocardial infarction using ultrasound images with DWT, GLCM and HOS methods: a comparative study. Comput Biol Med 62:86–93. https://doi.org/10.1016/j.compbiomed.2015.03.033
80. Wagner F, Gryanik A, Schulz-Wendtland R et al (2012) 3D characterization of texture: evaluation for the potential application in mammographic mass diagnosis. Biomed Eng (NY) 57:490–493
81. Wang S, Kim S, Chawla S et al (2010) Differentiation between glioblastomas and solitary brain metastases using diffusion tensor imaging. Neuroimage 44:653–660
82. Wang S, Zhang Y, Dong Z et al (2015) Feed-forward neural network optimized by hybridization of PSO and ABC for abnormal brain detection. Int J Imaging Syst Technol 25:153–164
83. Xu Y, van Beek EJR, Hwanjo Y et al (2006) Computer-aided classification of interstitial lung diseases via MDCT: 3D adaptive multiple feature method (3D AMFM). Acad Radiol 13:969–978
84. Yang X-S (2010) A new metaheuristic bat-inspired algorithm. In: Nat. inspired Coop. Strateg. Optim. (NICSO 2010). Springer, pp 65–74
85. Yang M-S, Chen C-H (1998) On the edited fuzzy K-nearest neighbor rule. IEEE Trans Syst Man, Cybern Part B 28:461–466
86. Yang X-S, Deb S (2009) Cuckoo search via Levy flights. In: Nat. Biol. Inspired Comput. 2009. NaBIC 2009. World Congr. pp 210–214
87. Yang X-S, Deb S (2010) Engineering optimisation by cuckoo search. Int J Math Model Numer Optim 1: 330–343
88. Yang G, Zhang Y, Yang J et al (2016) Automated classification of brain images using wavelet-energy and biogeography-based optimization. Multimed Tools Appl 75:15601–15617
89. Yilmaz S, Kucuksille EU (2015) A new modification approach on bat algorithm for solving optimization problems. Appl Soft Comput 28:259–275
90. Zacharaki EI, Wang S, Chawla S, Soo D (2009) Classification of brain tumor type and grade using MRI texture and shape in a machine learning scheme. Magn Reson Med 62:1609–1618
91. Zhang Y, Wang S, Ji G, Dong Z (2013) An MR brain images classifier system via particle swarm optimization and kernel support vector machine. Sci World J 2013
92. Zhang Y-D, Jiang Y, Zhu W et al (2018) Exploring a smart pathological brain detection method on pseudo Zernike moment. Multimed Tools Appl 77:22589–22604
93. Zollner FG, Emblem KE, Schad LR (2012) SVM-based glioma grading: optimization by feature reduction analysis. J Med Phys 22:205–214

Taranjit Kaur received her B.Tech and M.Tech degree in Electronics and Communication Engineering from Guru Nanak Dev Engineering College, Ludhiana in the year 2010 and 2012. Recently, she completed her Ph.D. degree from Dr. B R Ambedkar National Institute of Technology, Jalandhar, Punjab, India in the domain of MR Image Processing. Her area of interest is Medical Image Processing including the application of the optimization algorithms for the medical image analysis.

Barjinder Singh Saini is currently working as a Professor in Department of Electronics and Communication Engineering, Dr. B R Ambedkar National Institute of Technology, Jalandhar. He has completed his Ph.D. degree from Electronics and Communication Engineering Department, NIT Jalandhar on Signal Processing of Heart Rate Variability in the year 2009. His research interest includes Biomedical Signal and Image Processing.

Savita Gupta is currently working as a Professor in Department of Computer Science and Engineering, University Institute of Engineering and Technology, Panjab University, Chandigarh. She completed her Ph.D. degree from PTU, Jalandhar in 2007 in the field of Ultrasound image processing. Her research interests include wavelet-based image processing, network security, image compression and denoising.

Affiliations

Taranjit Kaur [1] · Barjinder Singh Saini [1] · Savita Gupta [2]

Barjinder Singh Saini
sainibss@gmail.com

Savita Gupta
savita2k8@yahoo.com

[1] Department of Electronics and Communication Engineering, Dr B R Ambedkar National Institute of Technology Jalandhar, Punjab 144011, India

[2] Department of Computer Science and Engineering, University Institute of Engineering and Technology, Sector 25, Panjab University, Chandigarh, India